

Diffusion Path Analysis of Alloy 600's and Alloy 690's Passive Films and Understanding/Predicting Cation Release Rates

Thomas M. Devine

Department of Materials Science and Engineering
University of California
Berkeley

Acknowledgements

Electric Power Research Institute

P.H. Chou, Proj Mngr - *In situ* SERS Investigation of
Passive Films Formed on Alloys 600 and 690 in
PWR PW - SCC

Dennis Hussey, Proj Mngr - Analysis of Alloy 690
General Corrosion Using Diffusion Path Analysis

Review of Literature

It is reasonable to expect that the cation release rate critically depends on the identity of the alloy's passive film.

Review of Literature

It is reasonable to expect that the cation release rate critically depends on the identity of the alloy's passive film.

A large number of investigations have been conducted to determine the identity of the passive films of Alloy 600 and Alloy 690 in PWR PW.

Review of Literature

It is reasonable to expect that the cation release rate critically depends on the identity of the alloy's passive film.

A large number of investigations have been conducted to determine the identity of the passive films of Alloy 600 and Alloy 690 in PWR PW.

The results of these investigations have been conflicting.

Review of Literature

It is reasonable to expect that the cation release rate critically depends on the identity of the alloy's passive film.

A large number of investigations have been conducted to determine the identity of the passive films of Alloy 600 and Alloy 690 in PWR PW.

The results of these investigations have been conflicting.

We have identified 10 factors, grouped into three major types, as possible causes of the discrepancies.

Composition of the Environment

Duration of the Oxidation

Analytical Technique

Parameters that might affect film's identity and identification

Composition of the Environment

pH ($[Li^+]$, [B])

P(H_2)

$[Ni^{+2}]_{aq}$, $[Fe^{+z}]_{aq}$

Time of Oxidation

Laboratory Tests

minutes to thousands of hours

Steam Generator Tubing

tens of thousands of hours

Analytical Technique

In situ

RS, SERS, EIS, M-S

Ex situ

XRD, AES, XPS, TEM (bright field, electron diffraction, EDS), SEM, Photoelectrochemical

Summary

Any one or any group of the factors listed on the previous slide might be determinative, in whole or in part, of the identity of the film.

By searching for correlations between specific films and each of the above listed factors we have determined that the most important factor is the **composition of the environment**.

In other words, regardless of the duration of the oxidation (*for $t > 10 \text{ min}$*) and regardless of the technique used to analyze the film, the same identification will be made if the same environment is used.

Examples of Film Studies

**OXIDATION OF NI BASE ALLOYS IN PWR WATER:
OXIDE LAYERS AND ASSOCIATED DAMAGE TO THE BASE METAL
P. Combrade¹, P.M. Scott², M. Foucault¹, E. Andrieu³, P. Marcus⁴**

Proceedings of the 12th International Conference on
Environmental Degradation of Materials in Nuclear Power System – Water Reactors –
Edited by T.R. Allen, P.J. King, and L. Nelson TMS (The Minerals, Metals & Materials Society), 2005

MOHAMED SENNOUR(1)*, LOÏC MARCHETTI(2), FRANTZ MARTIN(2), STÉPHANE PERRIN(2), RÉGINE
MOLINS(1), MICHÈLE PIJOLAT⁽³⁾ Journal of Nuclear Materials, 2010, 402(2-3), 147-156,

LOÏC MARCHETTI(1), STÉPHANE PERRIN(1)*, YVES WOUTERS(2), MICHÈLE PIJOLAT⁽³⁾
Electrochimica Acta, 2010, 55(19), 5384-5392

“Surface Analysis of PWR SG Tubing Specimens,” EPRI 1018720,
A. Parsi, A. Beyers, R.L. DeVito, J. Deshon Proj. Mngr. April 2009

F. Wang and T.M. Devine, “*In Situ* SERS of Alloy 600 and Alloy 690 ‘s Passive Films Formed
in PWR PW.

**Quantitative Micro-Nano (QMN) Approach to Predicting SCC of
Fe-Cr-Ni Alloys, Idaho Nat'l Lab June 13-18, 2010**

D. Morton and N. Lewis, “TEM Investigation of Passive Films of Alloy 600 and Alloy 690

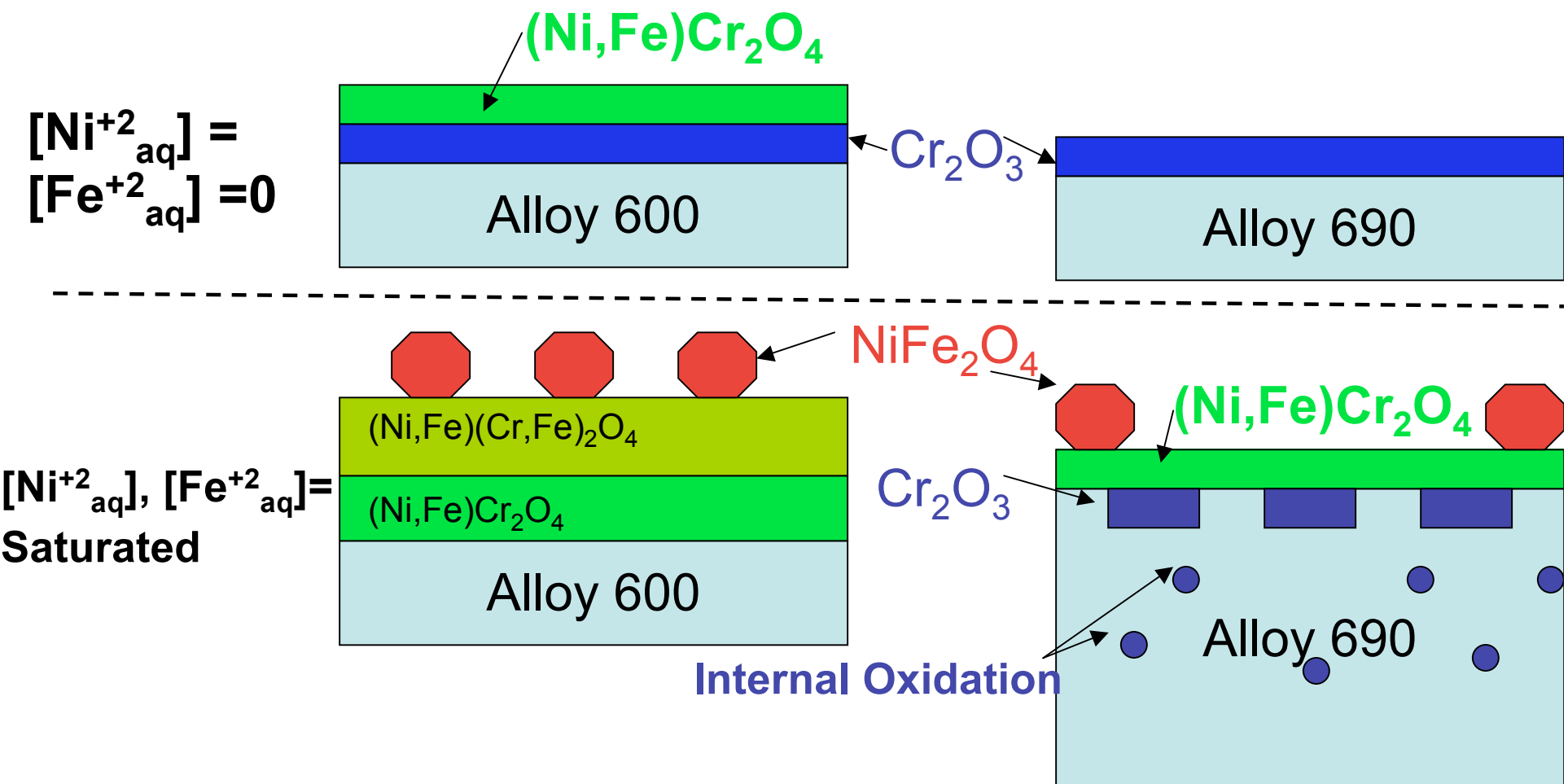
**Quantitative Micro-Nano (QMN) Approach to Predicting SCC of Fe-Cr-Ni Alloys,
Idaho Nat'l Lab June 13-18, 2010**

In summary,

there is near unanimous agreement in the literature that an outermost layer of nickel-ferrite crystallites forms on Alloy 600 and Alloy 690 when exposed to PWR PW saturated with Ni^{+2} and Fe^{+2} .

What we are reporting that is **new** is that the concentration of metal cations dissolved in PWR PW affects the identity of the innermost layer of film. This is an important finding because the corrosion resistance (cation release rate?) is critically dependent on the identity (composition and structure) of the innermost layer.

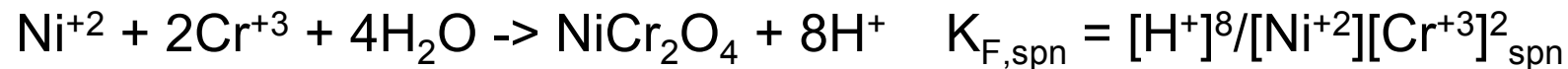
Microstructures Observed in Alloy 600 and Alloy 690 Oxidized in PWR PW



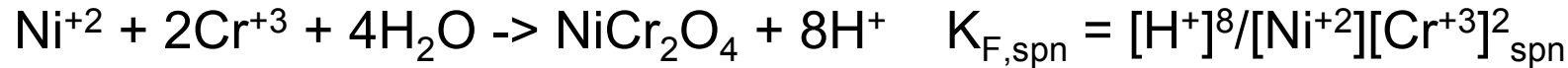
Explanations of the Influence of $[Ni^{+2}_{aq}]$ and $[Fe^{+2}_{aq}]$ on the Identities of the Inner Layer of Alloy 600's and Alloy 690's Film

- 1. Equilibria of Cr_2O_3 and $NiCr_2O_4$**
- 2. Diffusion Path Analyses of Composition/Structure of
Alloy/Oxide/Water Interphase.**

Explanation of the role of $[Ni^{+2}]_{aq}$ and $[Fe^{+2}]_{aq}$ on the identity (i.e., structure and composition) of the inner layer.



Explanation of the role of $[Ni^{+2}]_{aq}$ and $[Fe^{+2}]_{aq}$ on the identity (i.e., structure and composition) of the inner layer.



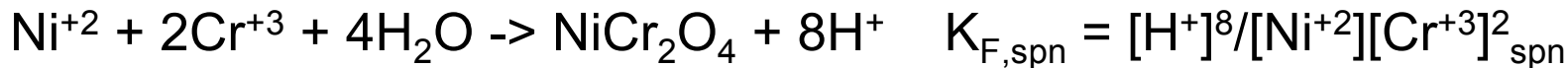
Thus,

$$[Cr^{+3}]_{crd}/[Cr^{+3}]_{spn} = (K_{F, spn}/K_{F, CRD})^{1/2} [Ni^{+2}]/[H^+]^2$$

To form spinel requires, $[Cr^{+3}]_{crd} > [Cr^{+3}]_{spn}$

i.e., $(K_{F, spn}/K_{F, CRD})^{1/2} > [H^+]^2/[Ni^{+2}]$

Explanation of the role of $[Ni^{+2}]_{aq}$ and $[Fe^{+2}]_{aq}$ on the identity (i.e., structure and composition) of the inner layer.



Thus,

$$[Cr^{+3}]_{crd}/ [Cr^{+3}]_{spn} = (K_{F, spn}/ K_{F, CRD})^{1/2} [Ni^{+2}]/ [H^+]^2$$

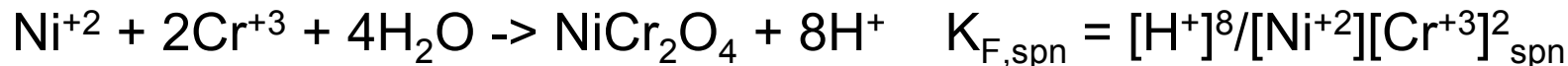
To form spinel requires, $[Cr^{+3}]_{crd} > [Cr^{+3}]_{spn}$
i.e., $(K_{F, spn}/ K_{F, CRD})^{1/2} > [H^+]^2/ [Ni^{+2}]$

In PWR PW at 325°C, $[H^+] = 10^{-7}$ M/l

$[Ni^{+2}]_{sat'd}$ is 3×10^{-9} M/l ; conservatively set $[Ni^{+2}]_{sat'd} = 10^{-9}$ M/l

Thus, to form spinel requires, $(K_{F, spn}/ K_{F, CRD}) > 10^4$

Explanation of the role of $[Ni^{+2}]_{aq}$ and $[Fe^{+2}]_{aq}$ on the identity (i.e., structure and composition) of the inner layer.



Thus,

$$[Cr^{+3}]_{crd}/ [Cr^{+3}]_{spn} = (K_{F, spn}/ K_{F, CRD})^{1/2} [Ni^{+2}]/ [H^+]^2$$

To form spinel requires, $[Cr^{+3}]_{crd} > [Cr^{+3}]_{spn}$

$$\text{i.e., } (K_{F, spn}/ K_{F, CRD})^{1/2} > [H^+]^2/ [Ni^{+2}]$$

In PWR PW at 325°C, $[H^+] = 10^{-7}$ M/l

$[Ni^{+2}]_{sat'd}$ is 3×10^{-9} M/l ; conservatively set $[Ni^{+2}]_{sat'd} = 10^{-9}$ M/l

Thus, to form spinel requires, $(K_{F, spn}/ K_{F, CRD}) > 10^4$



$$\Rightarrow (K_{F, spn}/ K_{F, CRD}) \sim 10^{16}, \text{ which is } \gg 10^4$$

$\Rightarrow [Ni^{+2}]_{aq} = [Ni^{+2}]_{sat'd}$ allows formation of $NiCr_2O_4$ inner layer rather than Cr_2O_3

Explanations of the Influence of $[Ni^{+2}_{aq}]$ and $[Fe^{+2}_{aq}]$ on the Identities of the Inner Layer of Alloy 600's and Alloy 690's Film

1. Equilibria of Cr_2O_3 and $NiCr_2O_4$
2. **Diffusion Path Analyses of Composition/Structure of Alloy/Oxide/Water Interphase.**

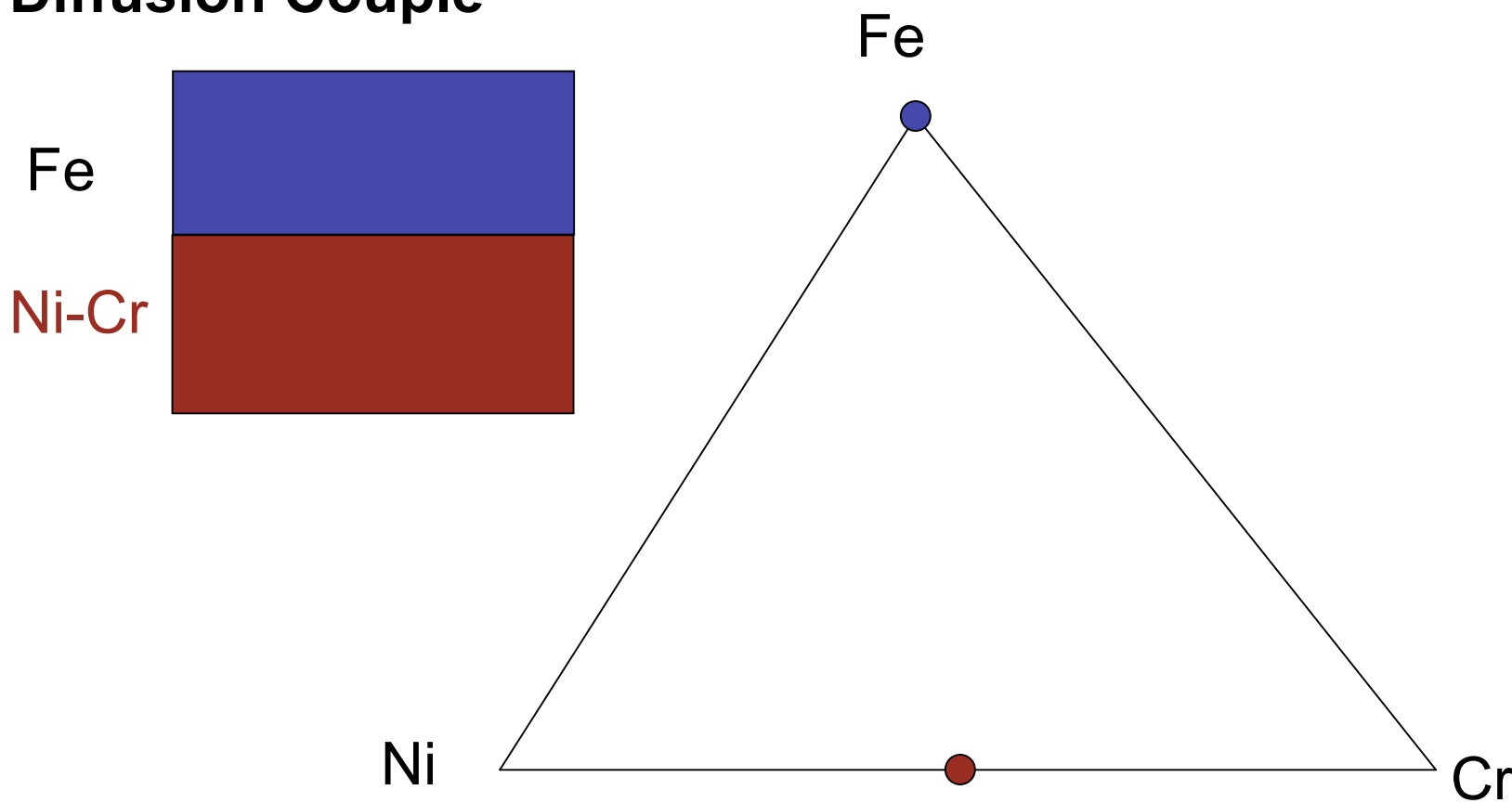
-Introduction to DPA

-DPA of Alloy 600's Film in PWR PW with $[Ni^{+2}_{aq}]$ and $[Fe^{+2}_{aq}] = 0$

- DPA of Alloy 690's Film in PWR PW with
(a) $[Ni^{+2}_{aq}]$ and $[Fe^{+2}_{aq}] = 0$ and
(b) $[Ni^{+2}_{aq}]$ and $[Fe^{+2}_{aq}]$ = saturated

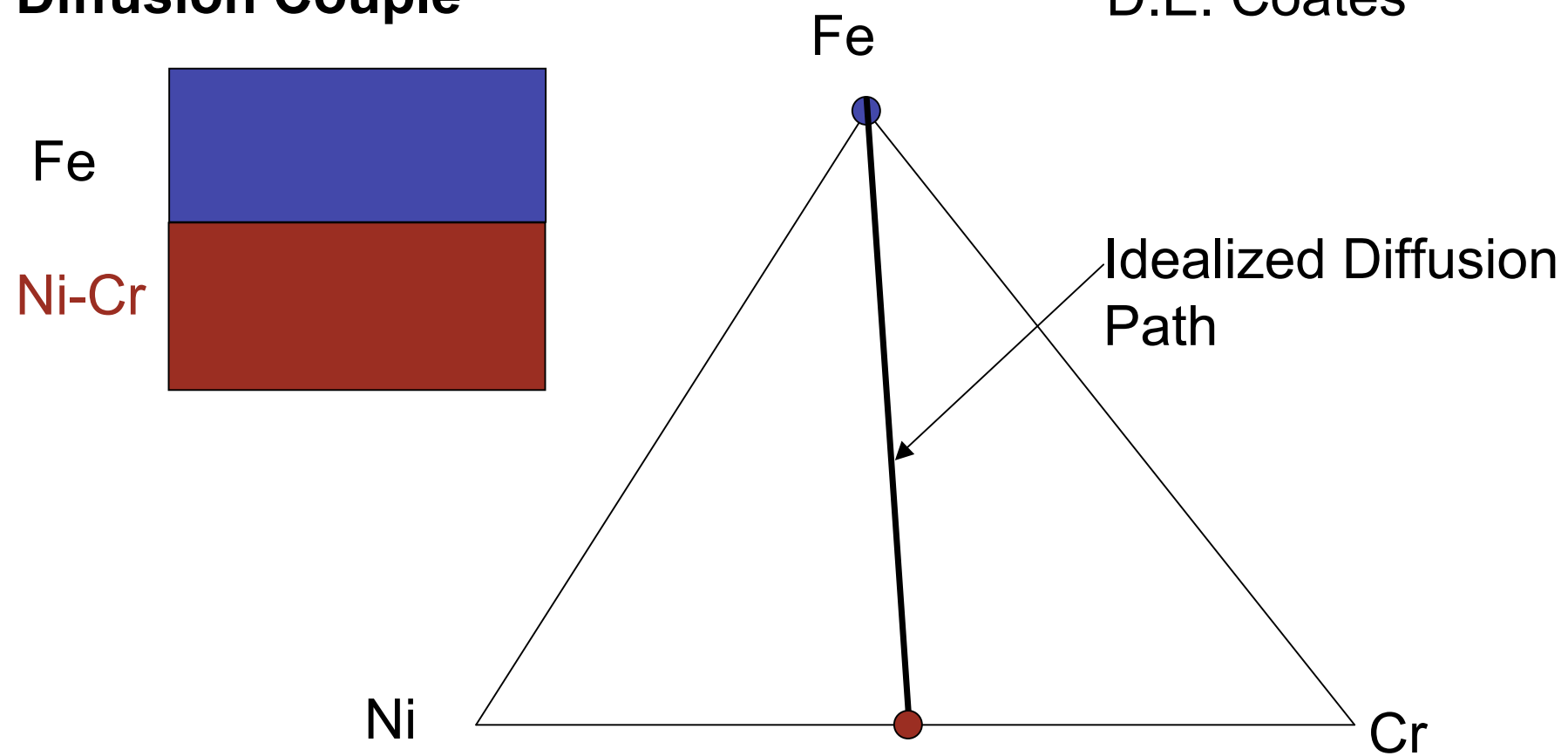
Diffusion Path Analyses - Rhines

Diffusion Couple



Diffusion Path Analyses - Rhines (~1940)

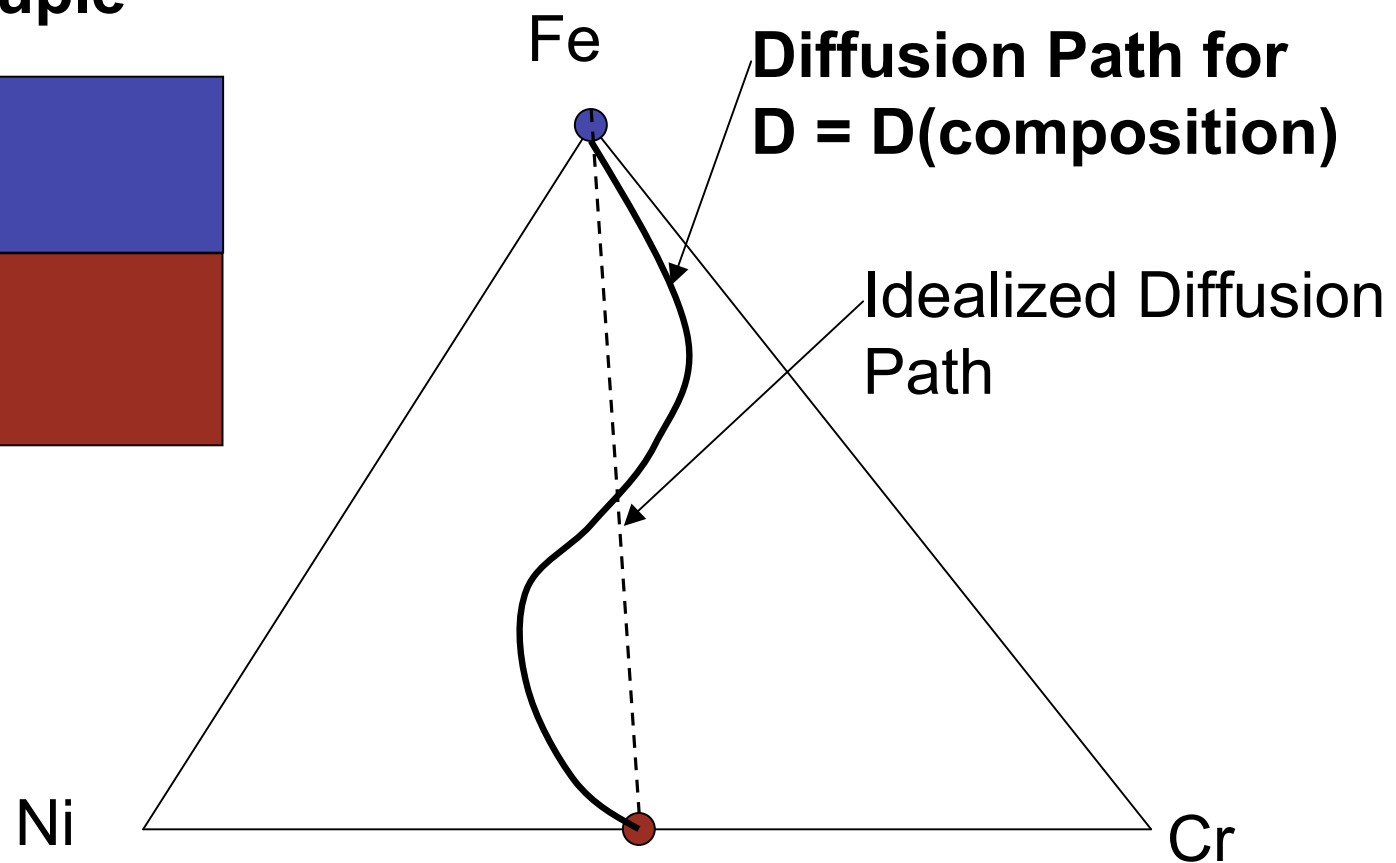
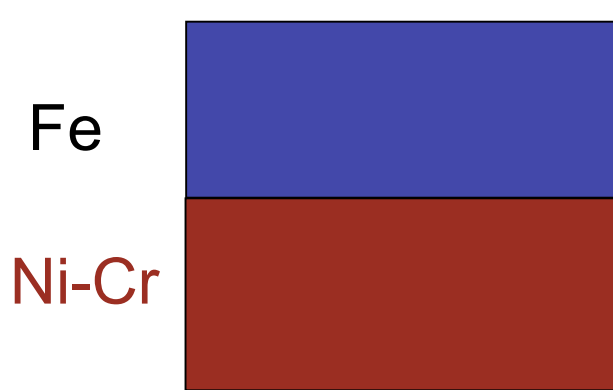
Diffusion Couple



Diffusion Path Analyses

J.S.Kirkaldy
D.E. Coates

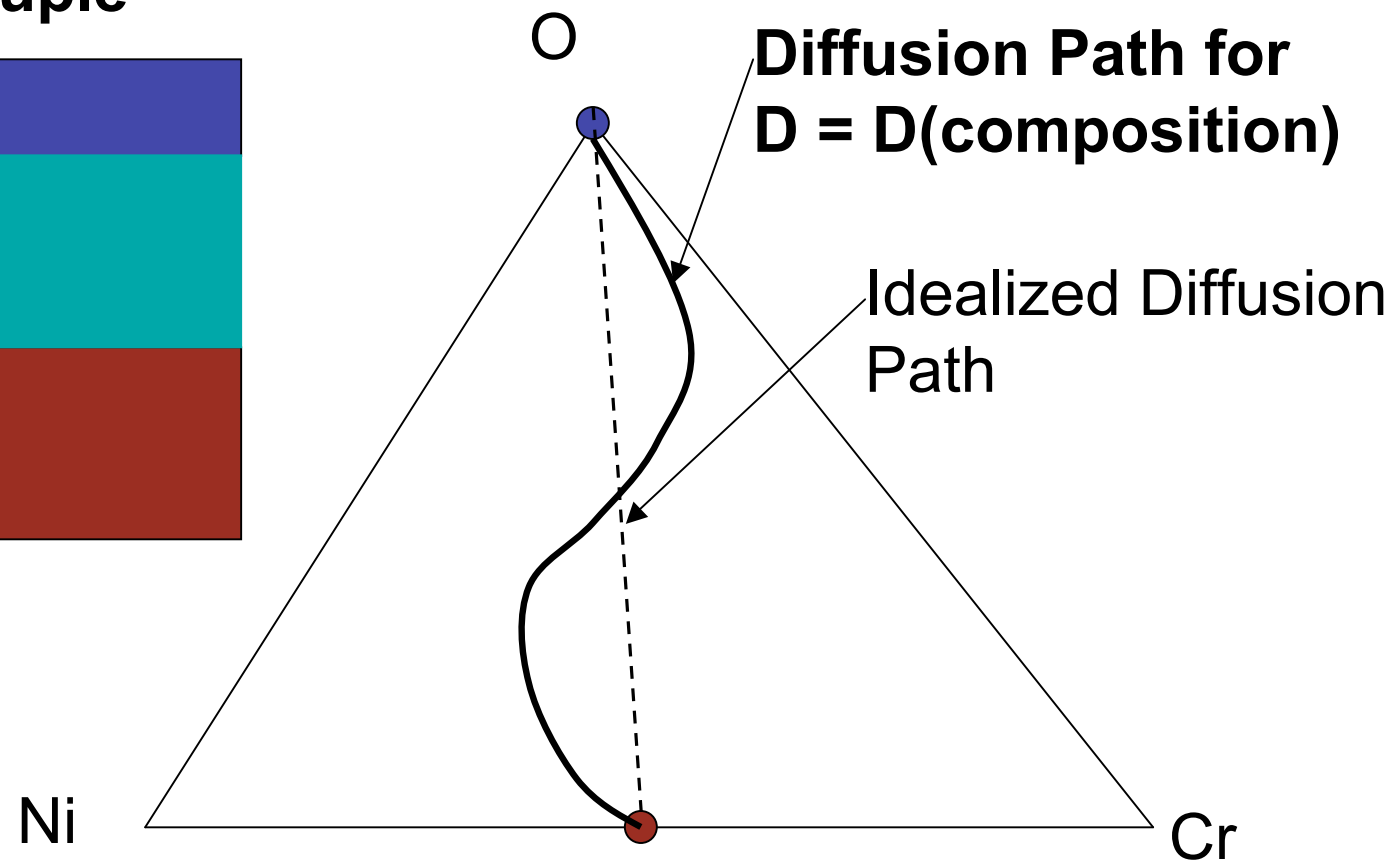
Diffusion Couple



Diffusion Path Analyses of Oxide Film Growth

Assumptions: Transport through the film is RDS
=> interfacial reactions are in equilibrium

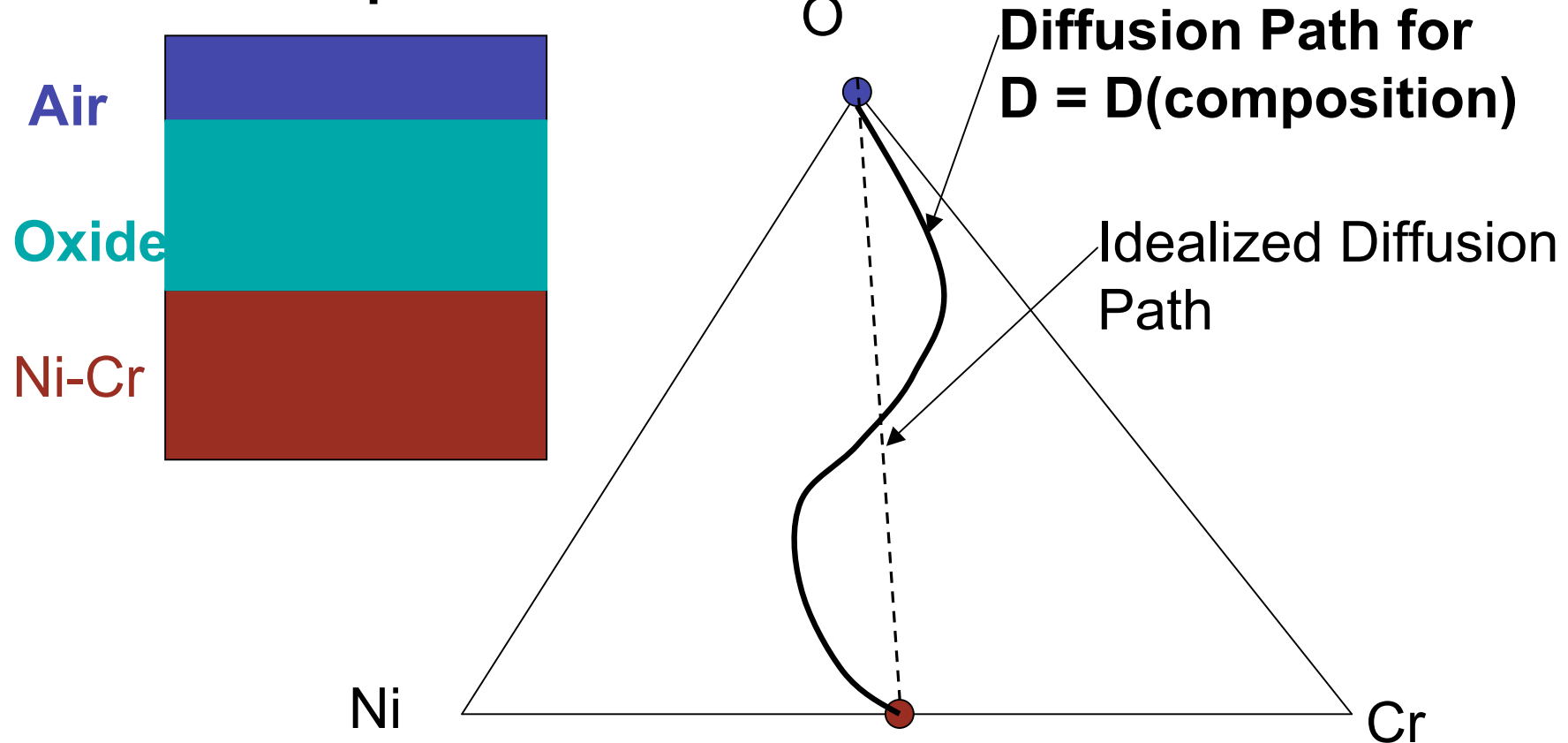
Diffusion Couple



Diffusion Path Analyses of Oxide Film Growth

Assumptions: Transport through the film is RDS
=> interfacial reactions are in equilibrium

Diffusion Couple

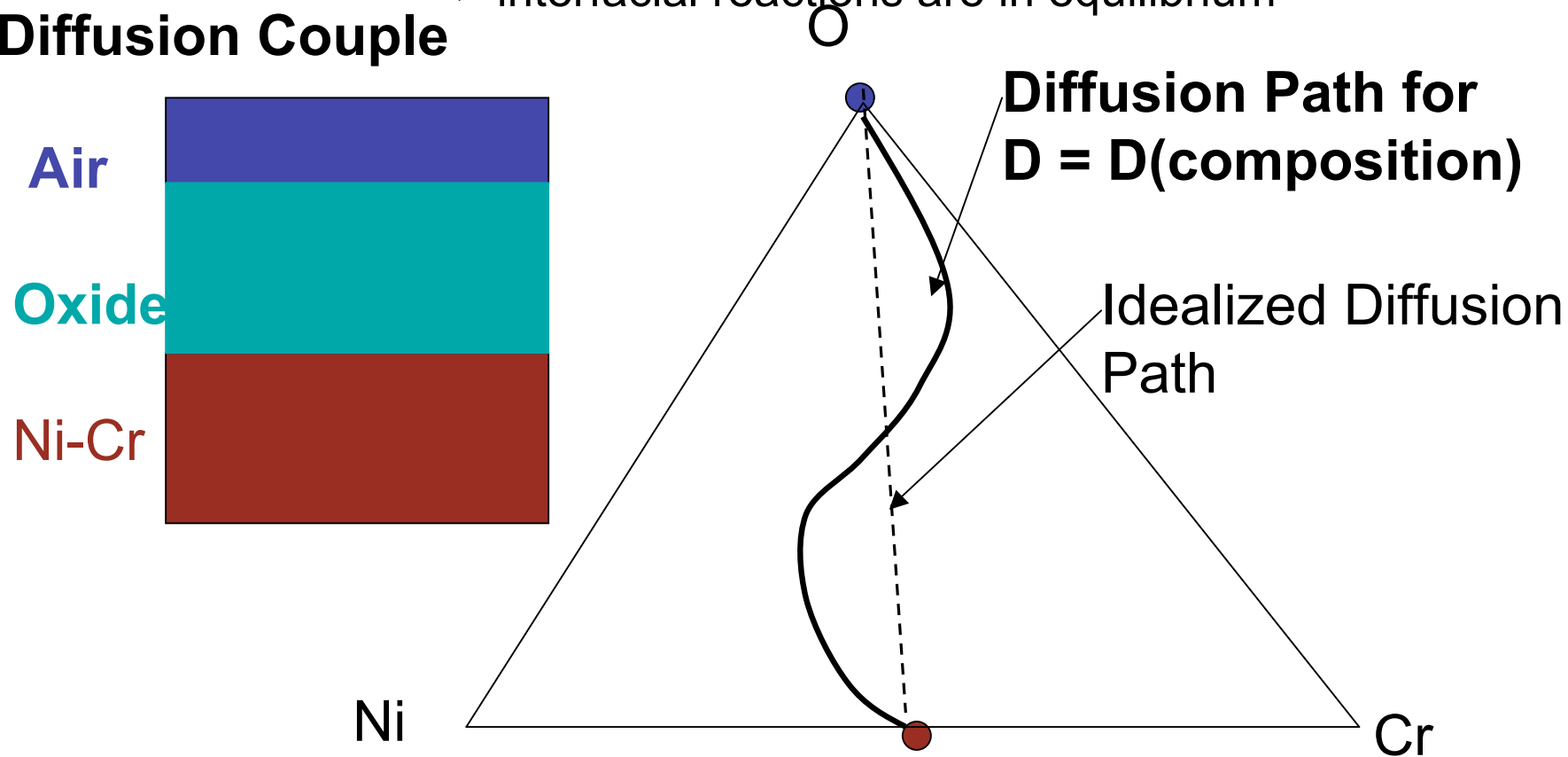


Thus, the complete microstructure of the surface is predicted from knowledge of (1) the ternary Ni-Cr-O phase diagram, and (2) the diffusivities of Ni, Cr, and O in each of the phases present in the phase diagram.

Diffusion Path Analyses of Oxide Film Growth

Assumptions: Transport through the film is RDS
=> interfacial reactions are in equilibrium

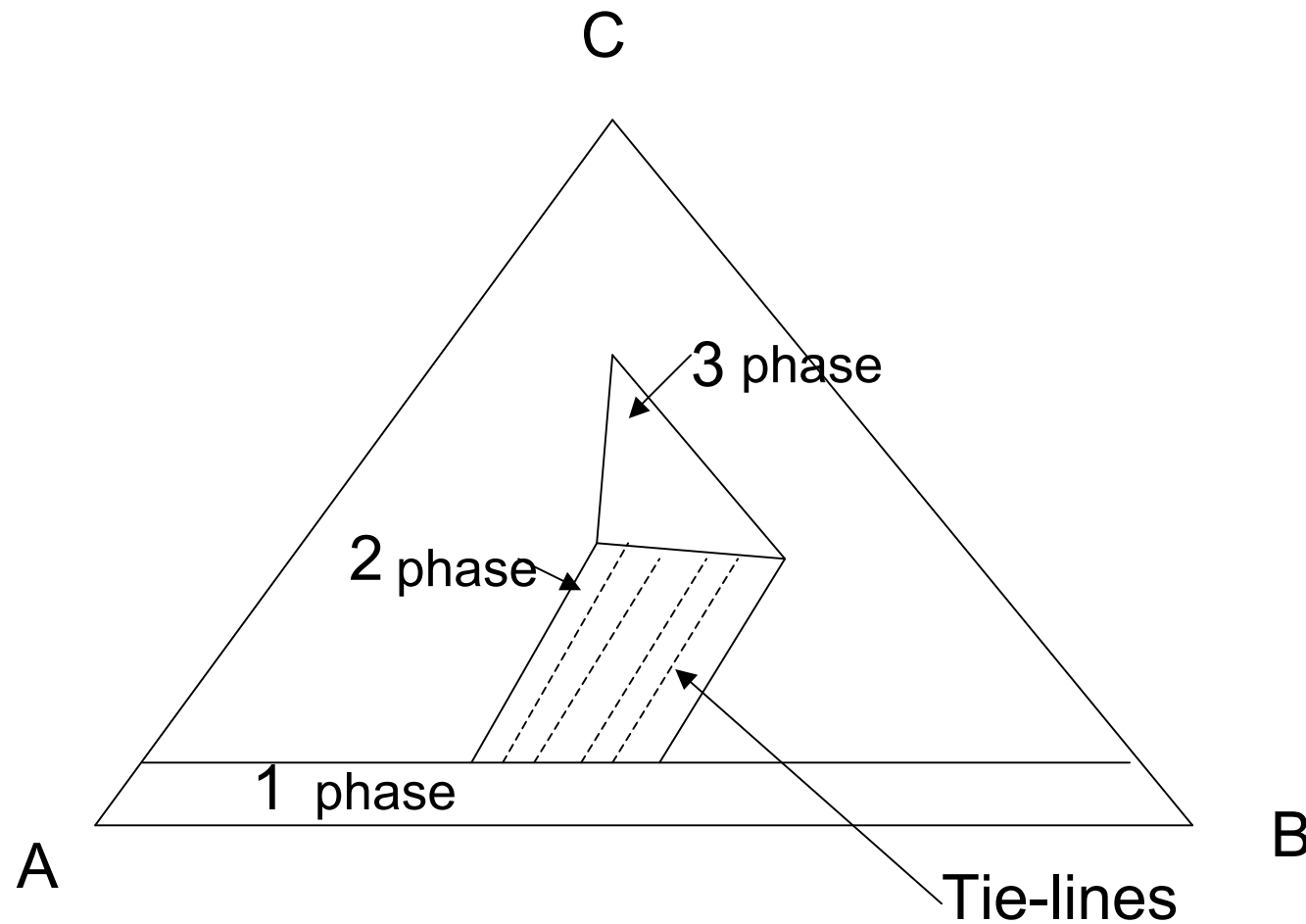
Diffusion Couple



For Alloys 600 and 690 in water at 320°C, we don't know the phase diagram or the diffusivities. However, important information about the film is obtained by measuring the species present in the film and plotting the results on an assumed phase diagram.

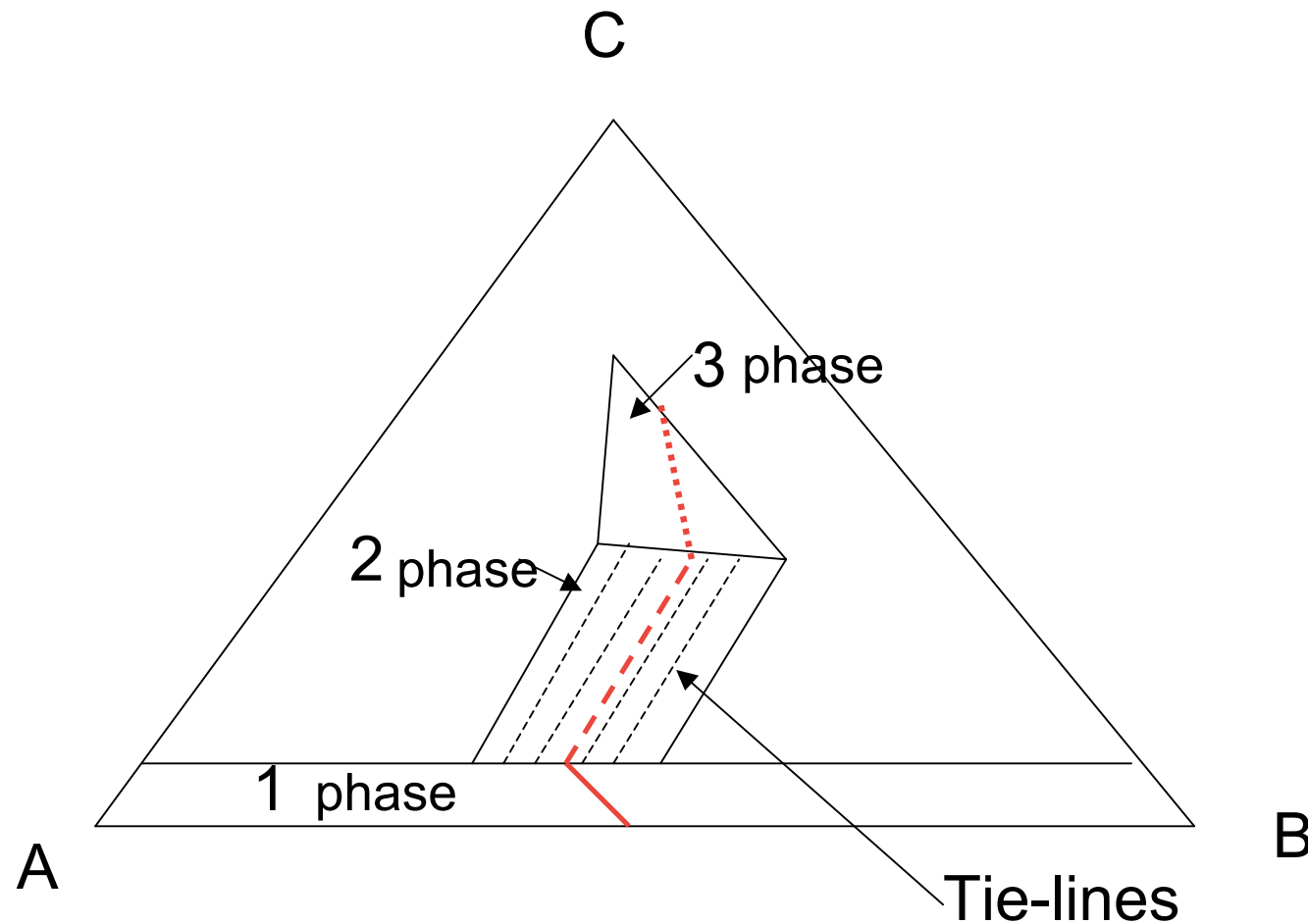
Introduction to DPA

Major “rule/theorems” as applied to oxidation of Ni-Cr-Fe



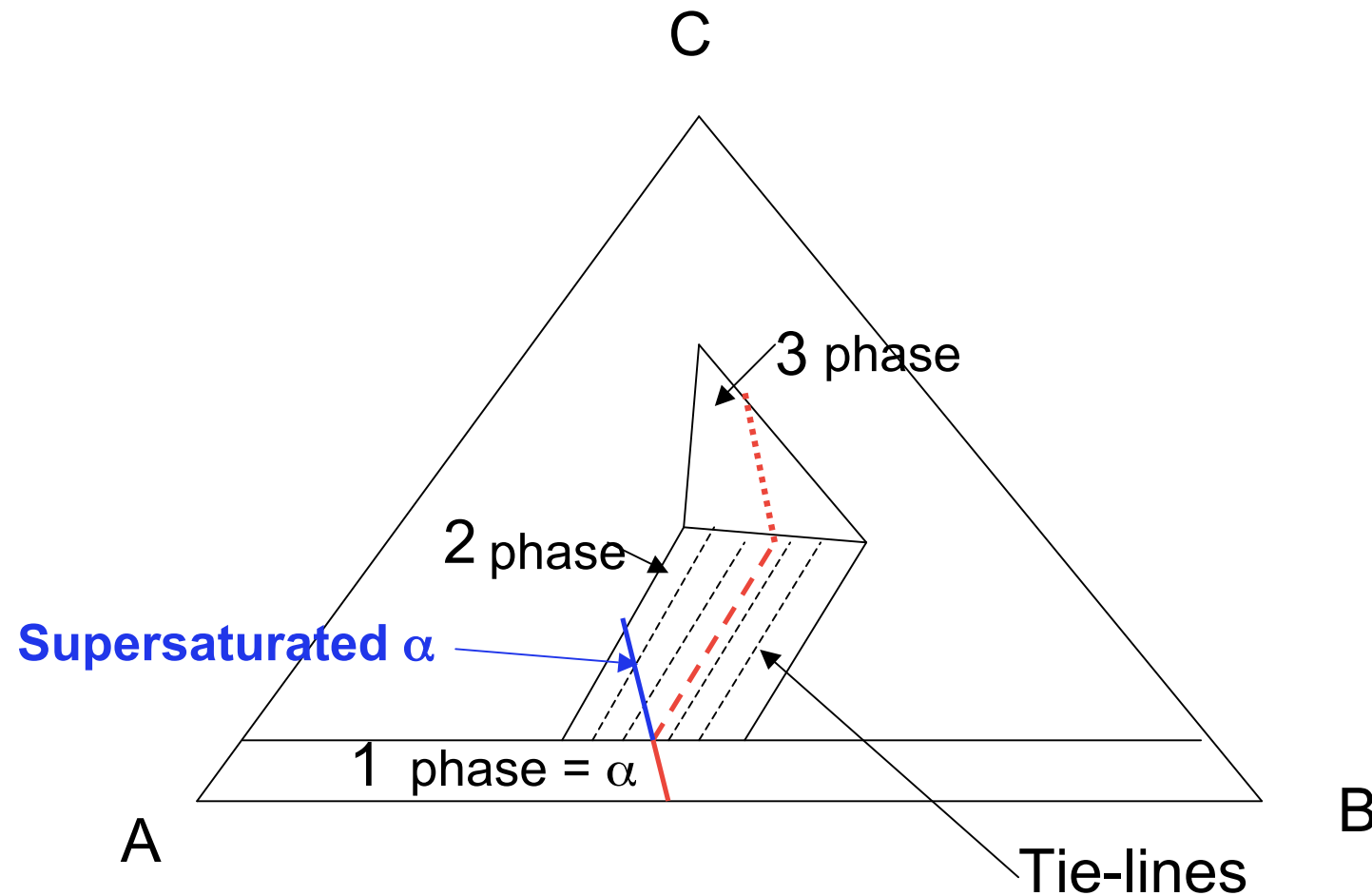
Introduction to DPA

Major “rule/theorems” as applied to oxidation of Ni-Cr-Fe



Introduction to DPA

Major “rule/theorems” as applied to oxidation of Ni-Cr-Fe



Explanations of the Influence of $[Ni^{+2}_{aq}]$ and $[Fe^{+2}_{aq}]$ on the Identities of the Inner Layer of Alloy 600's and Alloy 690's Film

1. Equilibria of Cr_2O_3 and $NiCr_2O_4$
2. **Diffusion Path Analyses of Composition/Structure of Alloy/Oxide/Water Interphase.**
 - Introduction to DPA
 - DPA of Alloy 600's Film in PWR PW with $[Ni^{+2}_{aq}]$ and $[Fe^{+2}_{aq}] = 0$**
 - DPA of Alloy 690's Film in PWR PW with
 - (a) $[Ni^{+2}_{aq}]$ and $[Fe^{+2}_{aq}] = 0$ and
 - (b) $[Ni^{+2}_{aq}]$ and $[Fe^{+2}_{aq}]$ = saturated

Hypothesized Ni-Cr-Water Ternary Phase Diagram* at 300°C

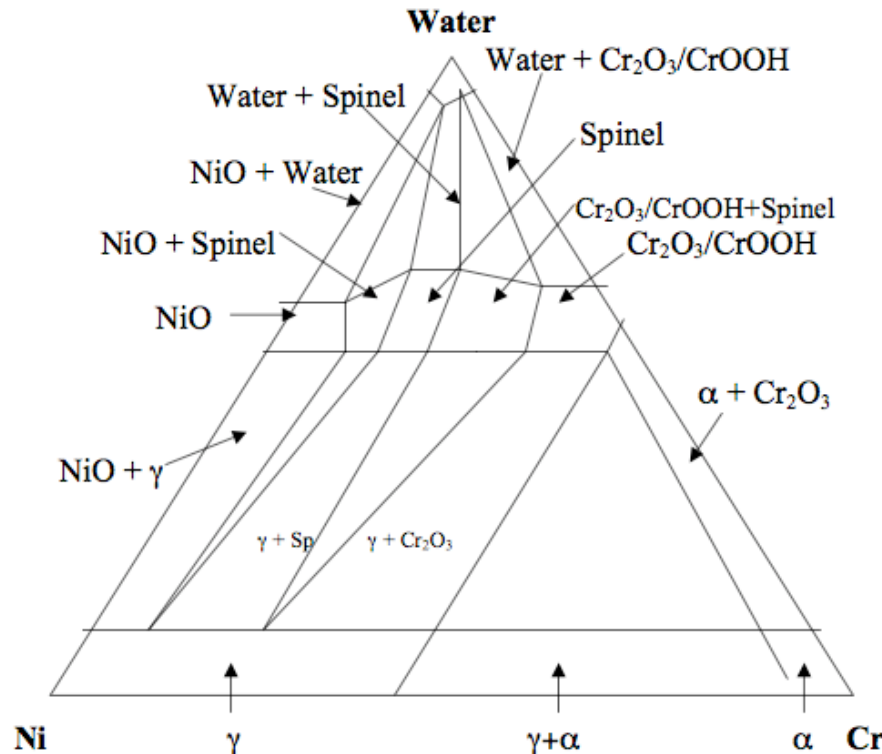


Figure 1. Hypothetical ternary Ni-Cr-Water phase diagram at 300°C.

NB - diagram is significantly distorted

* Based on Ni-Cr-O at 1000°C, Croll and Wallwork

Ni-Cr-Water Ternary Phase Diagram

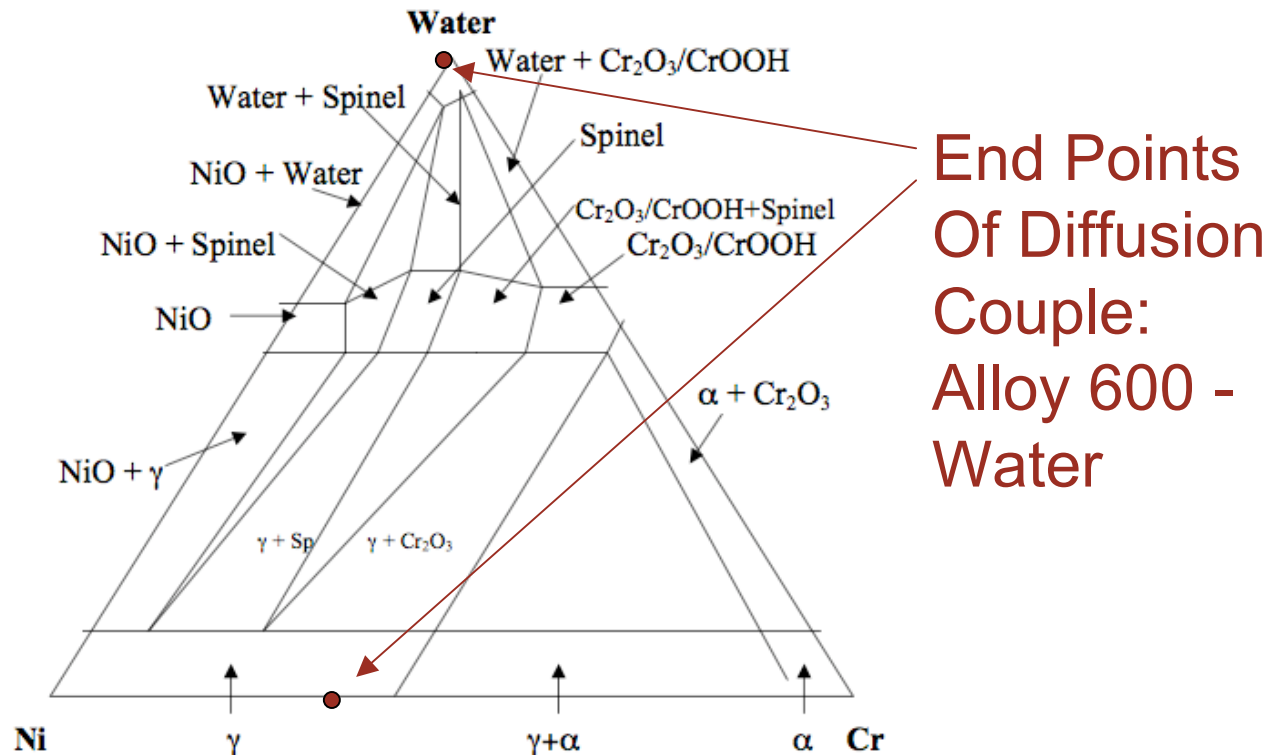
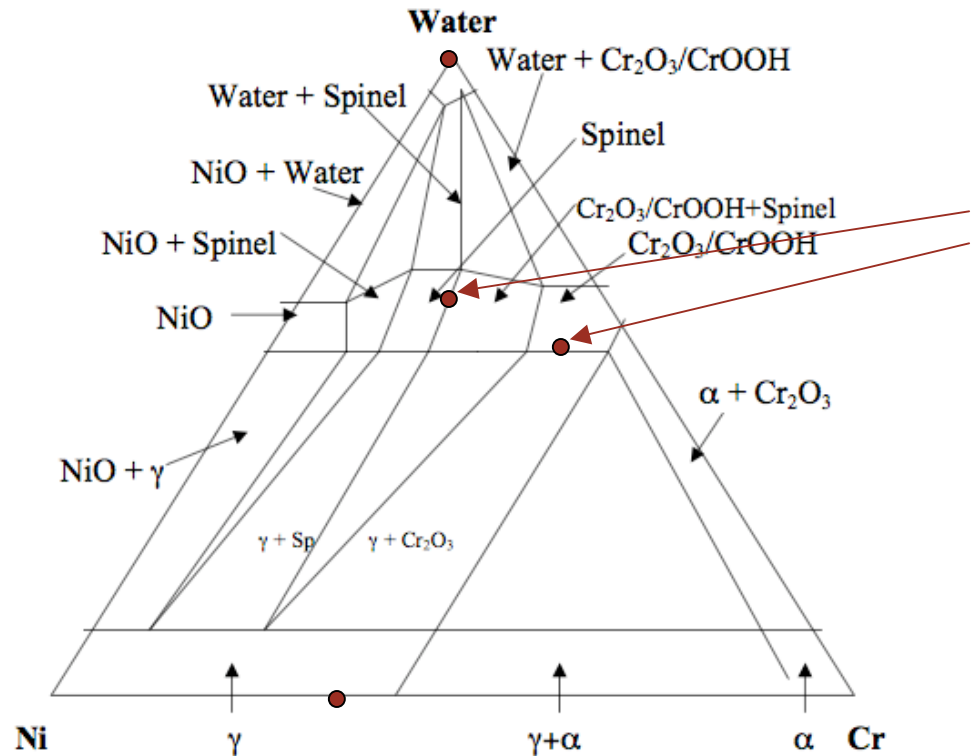


Figure 1. Hypothetical ternary Ni-Cr-Water phase diagram at 300°C.

Ni-Cr-Water Ternary Phase Diagram



SERS and
TEM of
Alloy 600

Figure 1. Hypothetical ternary Ni-Cr-Water phase diagram at 300°C.

Ni-Cr-Water Ternary Phase Diagram

Construction of Diffusion Path

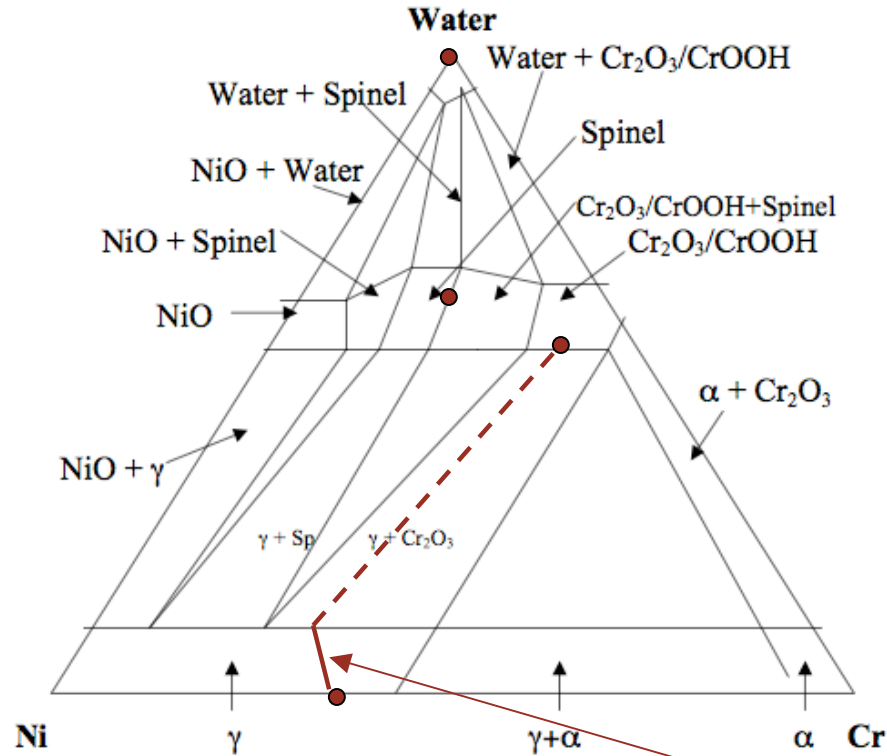
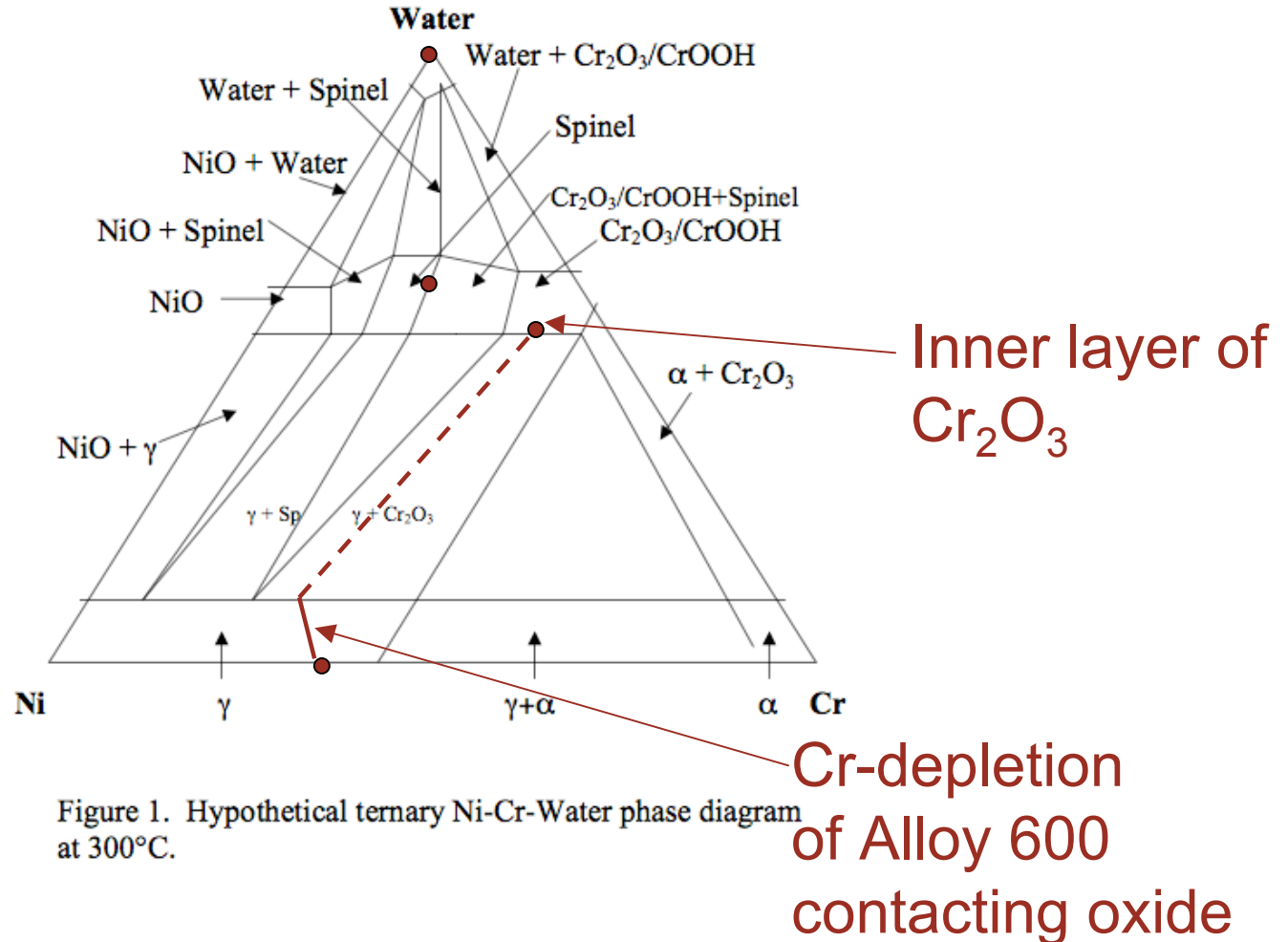


Figure 1. Hypothetical ternary Ni-Cr-Water phase diagram
at 300°C.

Cr-depletion
of Alloy 600
contacting oxide

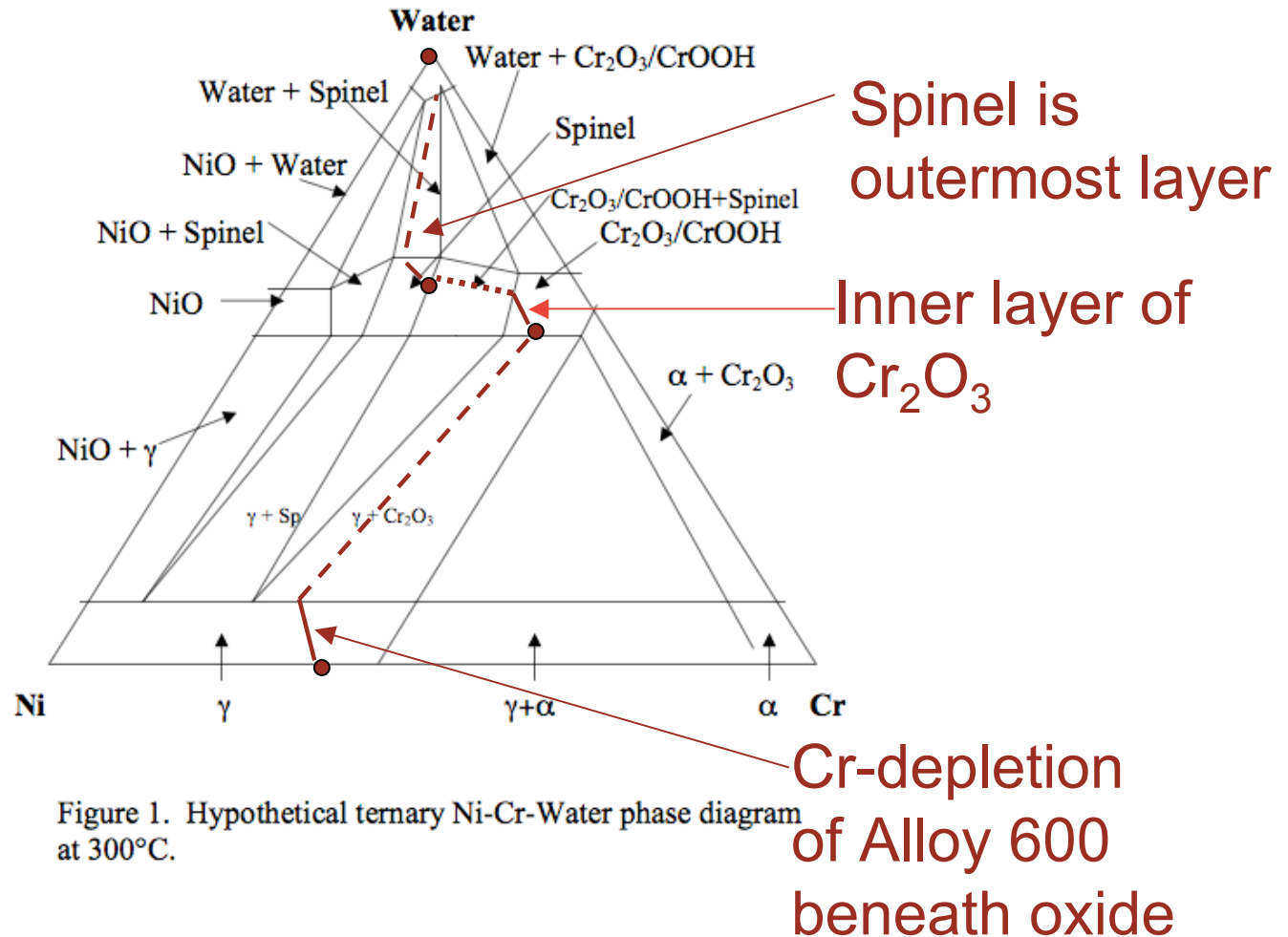
Ni-Cr-Water Ternary Phase Diagram

Construction of Diffusion Path



Ni-Cr-Water Ternary Phase Diagram

Construction of Diffusion Path



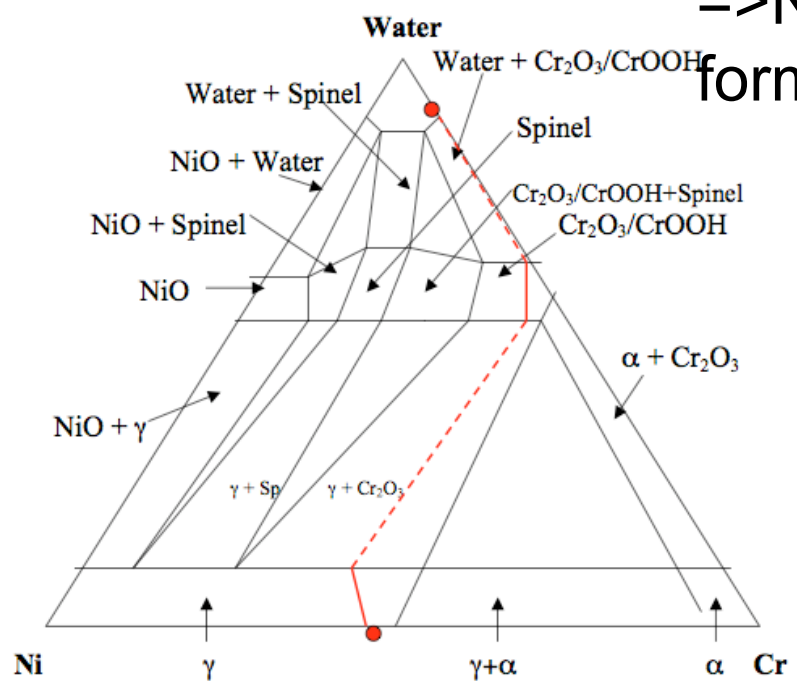
Explanations of the Influence of $[Ni^{+2}_{aq}]$ and $[Fe^{+2}_{aq}]$ on the Identities of the Inner Layer of Alloy 600's and Alloy 690's Film

1. Equilibria of Cr_2O_3 and $NiCr_2O_4$
2. Diffusion Path Analyses of Composition/Structure of Alloy/Oxide/Water Interphase.
 - Introduction to DPA
 - DPA of Alloy 600's Film in PWR PW with $[Ni^{+2}_{aq}]$ and $[Fe^{+2}_{aq}] = 0$
 - **DPA of Alloy 690's Film in PWR PW with**
 - (a) $[Ni^{+2}_{aq}]$ and $[Fe^{+2}_{aq}] = 0$ and
 - (b) $[Ni^{+2}_{aq}]$ and $[Fe^{+2}_{aq}]$ = saturated

Alloy 690 in PWR PW with

$$[\text{Ni}^{+2}_{\text{aq}}] = [\text{Fe}^{+2}_{\text{aq}}] = 0$$

=> NiCr_2O_4 and $(\text{Ni},\text{Fe})\text{Cr}_2\text{O}_4$ cannot form



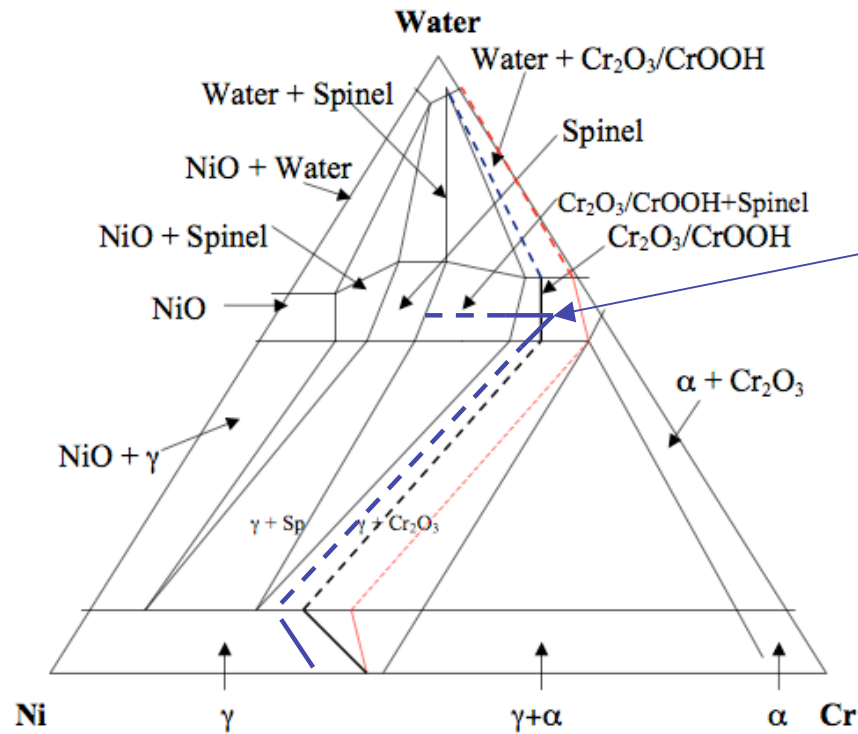
- End points of diffusion couple

— DP in single phase region

DP #1 – RED – $[\text{Ni}^{+2}_{\text{aq}}] = [\text{Fe}^{+2}_{\text{aq}}] = 0$

----- DP in two phase region

Comparison of Diffusion Paths of Alloy 690 and Alloy 600



Approximately
no [O⁼] gradient
in Cr₂O₃ of
Alloy 600

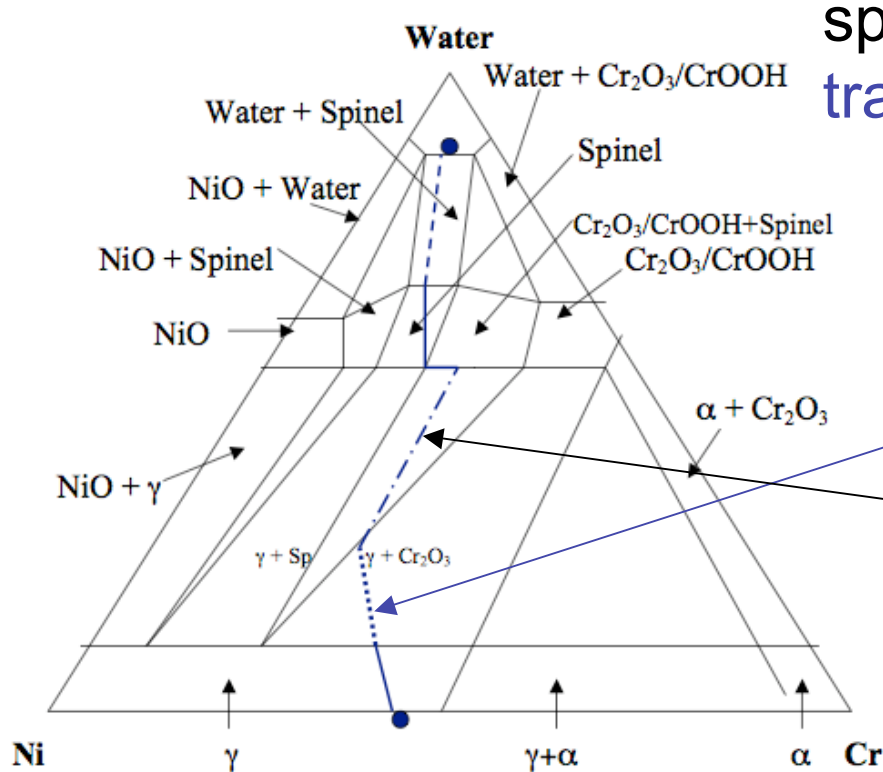
Figure 41. Two diffusion paths (DP) of Alloy 690. The DP at 300°C is colored red. The DP at 320°C is colored blue.

At 320°C, DPA => Alloy 690's film is a consequence of (1) the alloy's high [Cr], and (2) the growth of Cr₂O₃ is controlled by O⁼ diffusion.

Explanations of the Influence of $[Ni^{+2}_{aq}]$ and $[Fe^{+2}_{aq}]$ on the Identities of the Inner Layer of Alloy 600's and Alloy 690's Film

1. Equilibria of Cr_2O_3 and $NiCr_2O_4$
2. Diffusion Path Analyses of Composition/Structure of Alloy/Oxide/Water Interphase.
 - Introduction to DPA
 - DPA of Alloy 600's Film in PWR PW with $[Ni^{+2}_{aq}]$ and $[Fe^{+2}_{aq}] = 0$
 - **DPA of Alloy 690's Film in PWR PW with**
 - (a) $[Ni^{+2}_{aq}]$ and $[Fe^{+2}_{aq}] = 0$ and
 - (b) $[Ni^{+2}_{aq}]$ and $[Fe^{+2}_{aq}] = \text{saturated}$**

$[Ni^{+2}_{aq}], [Fe^{+2}_{aq}]$ = saturation and allows $(Ni, Fe)Cr_2O_4$ to form



spinel, $(Ni, Fe)Cr_2O_4$, allows rapid transport of O into the alloy

High O concentration in the alloy leads to internal oxidation

and a complex interface of $\gamma+Cr_2O_3 // Cr_2O_3+Ni, Fe)Cr_2O_4$

Continuous layer of Cr_2O_3 does not form because diffusion of Cr is very low compared to Diffusion of O

DP#2 – BLUE - $[Ni^{+2}_{aq}] = [Fe^{+2}_{aq}]$ = saturation

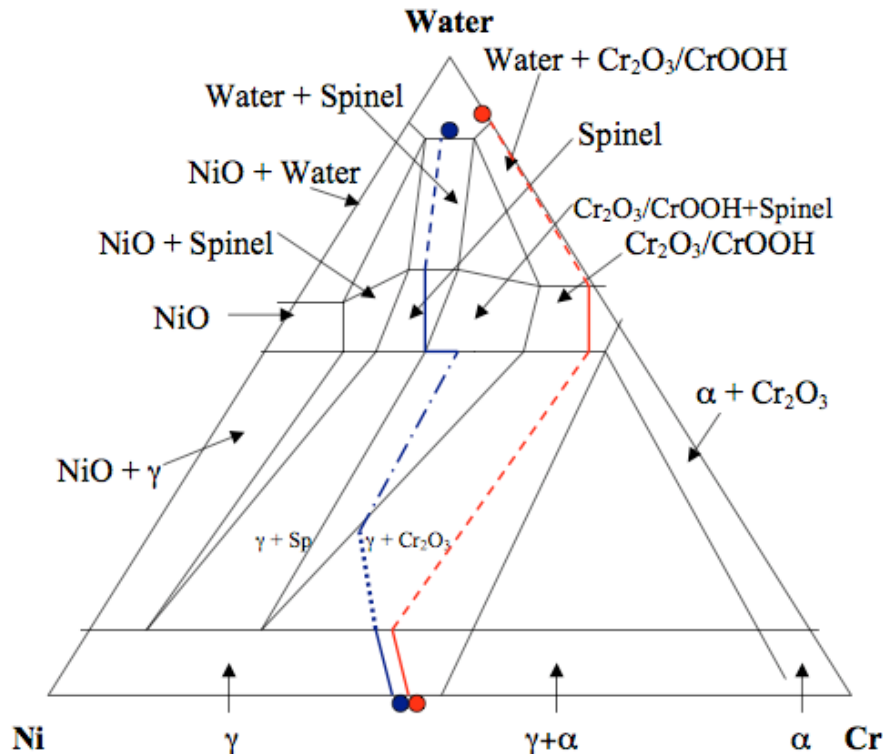
Thus: key feature is the formation of spinel, $(Ni, Fe)Cr_2O_4$, which allows rapid transport of O into the alloy

Film Identity and Cation Release

Influence of $[Ni^{+2}_{aq}]$ and $[Fe^{+2}_{aq}]$ on Cation Release

High $[Ni^{+2}_{aq}]$ and $[Fe^{+2}_{aq}]$

allows $(Ni,Fe)Cr_2O_4$ to form as inner layer.
 $(Ni,Fe)Cr_2O_4$ does not block O leading to high [O] in Alloy.
 High [O] and slow diffusion of Cr in alloy causes internal oxidation, Cr_2O_3 , and the absence of a continuous layer of Cr_2O_3
 High cation diffusion in $(Ni,Fe)Cr_2O_4$ causes high Cation Release.

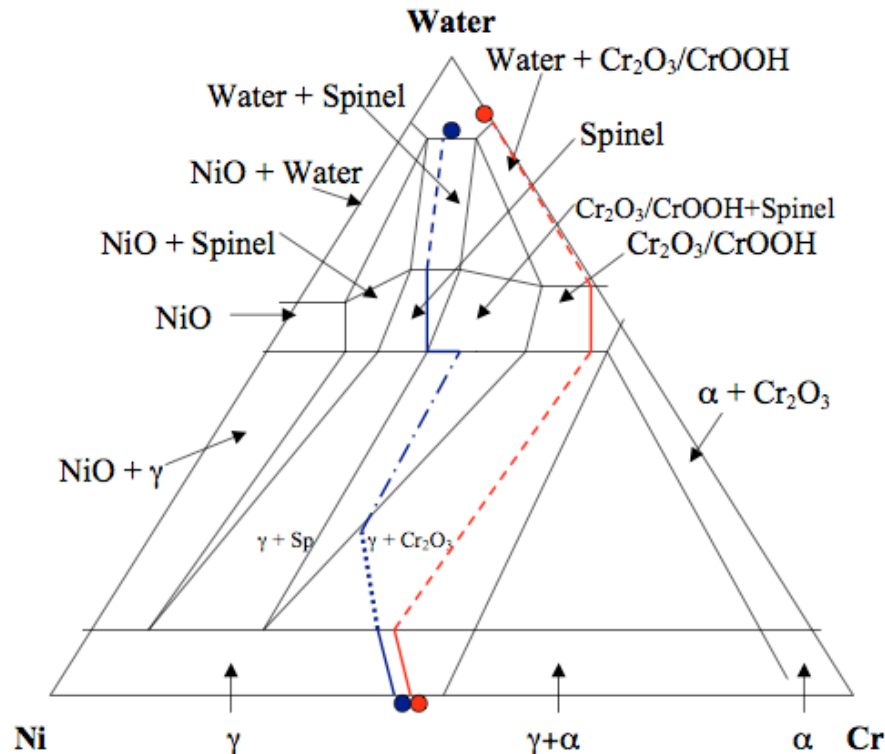


$$DP\#1 - RED - [Ni^{+2}_{aq}] = [Fe^{+2}_{aq}] = 0$$

$$DP\#2 - BLUE - [Ni^{+2}_{aq}] = [Fe^{+2}_{aq}] = \text{saturation}$$

Influence of $[Ni^{+2}_{aq}]$ and $[Fe^{+2}_{aq}]$ on Cation Release

$$[Ni^{+2}_{aq}] \text{ and } [Fe^{+2}_{aq}] = 0$$



DP #1 – RED – $[Ni^{+2}_{aq}] = [Fe^{+2}_{aq}] = 0$

DP#2 – BLUE - $[Ni^{+2}_{aq}] = [Fe^{+2}_{aq}] = \text{saturation}$

prevents $(Ni,Fe)Cr_2O_4$ from forming and Cr_2O_3 forms as an inner layer.
 Cr_2O_3 blocks O leading to low [O] in Alloy and prevents internal oxidation.
The continuous layer of Cr_2O_3 inhibits cation diffusion and Cation Release.

Hypothesized Relationship of Film's Identity to Cation Release

Inner layer of Cr₂O₃ blocks O transport to alloy and inhibits cation transport to aqueous phase.

In PWR PW with [Ni⁺²_{aq}] = [Fe⁺²_{aq}] = 0

Layer of Cr₂O₃ forms on Alloy 690

Inner layer of Cr₂O₃ forms on Alloy 600

In PWR PW with [Ni⁺²_{aq}] = [Fe⁺²_{aq}] = saturation

Alloy 690- Inner layer of (Ni,Fe)Cr₂O₄ on top of discontinuous Cr₂O₃

Alloy 600 - Inner layer of (Ni,Fe)Cr₂O₄

=>Lowest cation release from Alloy 690 in PWR PW, with [Ni⁺²_{aq}] = [Fe⁺²_{aq}] = 0

Proposed Work

Use TEM to verify the DPA

Develop quaternary Ni-Cr-Fe-Water Phase Diagram

calculate

measure

plot DPs (obtained from analytical TEM)

Develop/measure expressions for oxidation rate, film growth rate, cation release rate for each interfacial microstructure

Experimentally confirm role of aq Ni^{+2} and Fe^{+z} on inner layer.

Will inner layer change (kinetic demixing) if water's cation concentrations change?

Properties of film that might affect cation release rate

We've emphasized the importance of Alloy composition and Water Chemistry on Film Identity and Cation Release rate. There are other parameters to consider:

Electrical conductivity (carrier density)

n-type vs p-type

Band gap

Ionic conductivity

anion and cation transport coefficients

Film's grain size, grain shape, and grain orientation

Proposal/continued

We've emphasized the importance of Alloy composition and Water Chemistry on Film Identity and Cation Release rate. There are other parameters to consider:

Emphasize importance of short circuit diffusion through Oxide - esp GB diffusion.

Investigate film microstructure (i.e., gs, g orientation, g shape anisotropy) of Alloy 600, Alloy 690 as f(t) and as f(aqNi⁺² and Fe⁺²). How does gs etc of inner layer (IL) of Cr₂O₃ compare to gs of inner layer of Spinel? How does gs of OL of sp compare to gs of IL of spinel?

What might be done to affect the gs of the IL?

How important is GS relative to the chemical identity of the Oxide IL? A fine grain IL of spinel might be more protective vs film growth and cation release than an IL of coarse grained Cr₂O₃.

By virtue of their different mechanisms of formation, is the GS of Cr₂O₃ inherently different (i.e., grain size, grain orientation) than the GS of an IL of spinel?

Measure film growth rate and cation release rate as a f of gr size for IL of Cr₂O₃ vs IL of Spinel

What is mechanism of cation release? E.g., is it primarily by GB diffusion of cations through the oxide? Or is it primarily by bulk diffusion of cations through the oxide?

Is cation release related to chemical dissolution of the oxide?

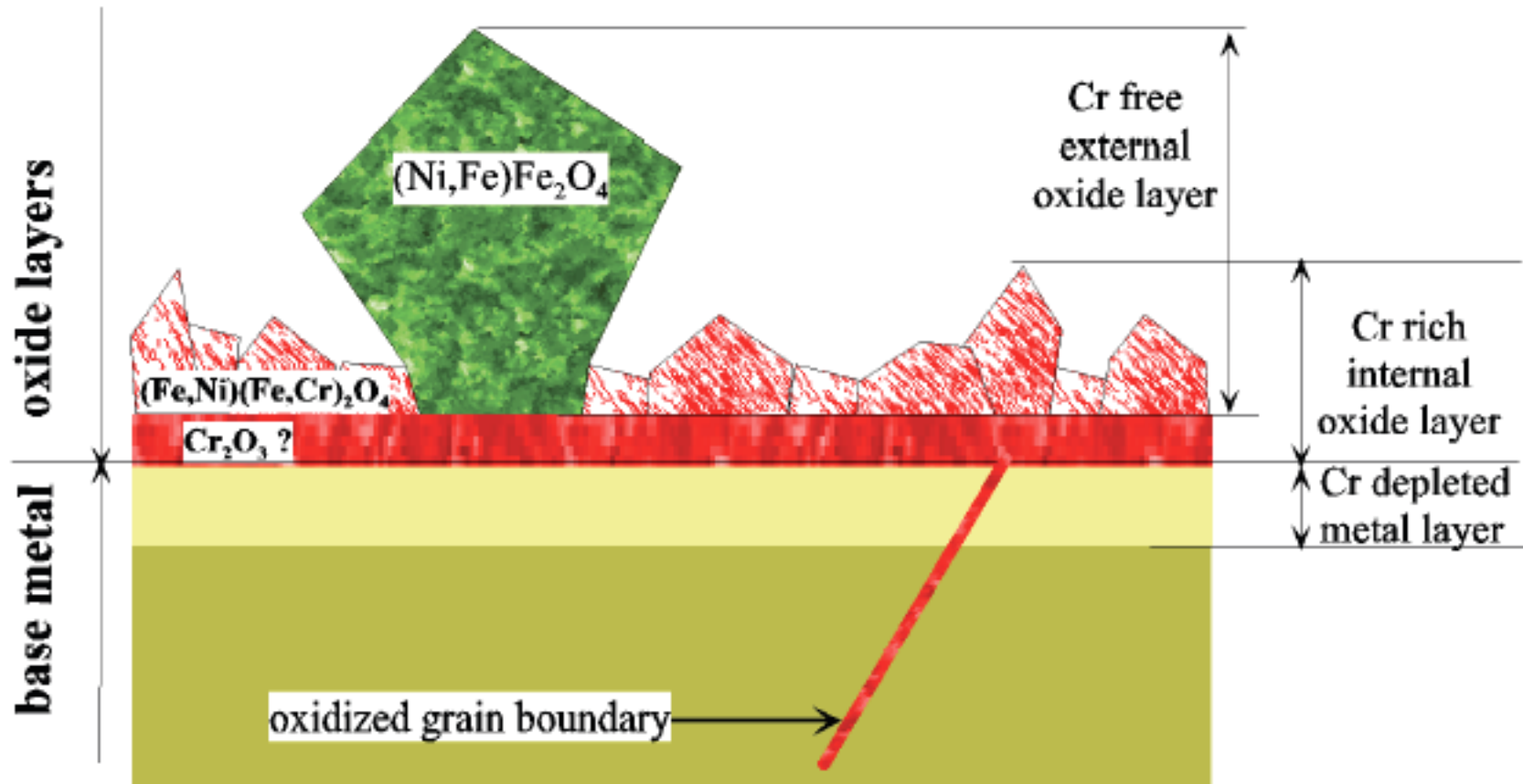
Illustrative examples of Film Investigations are presented
in the next 12 slides

Our New Analysis points out the critical role of aqueous metal cations on the structure and composition of the Inner Layer of passive film.

Specifically,

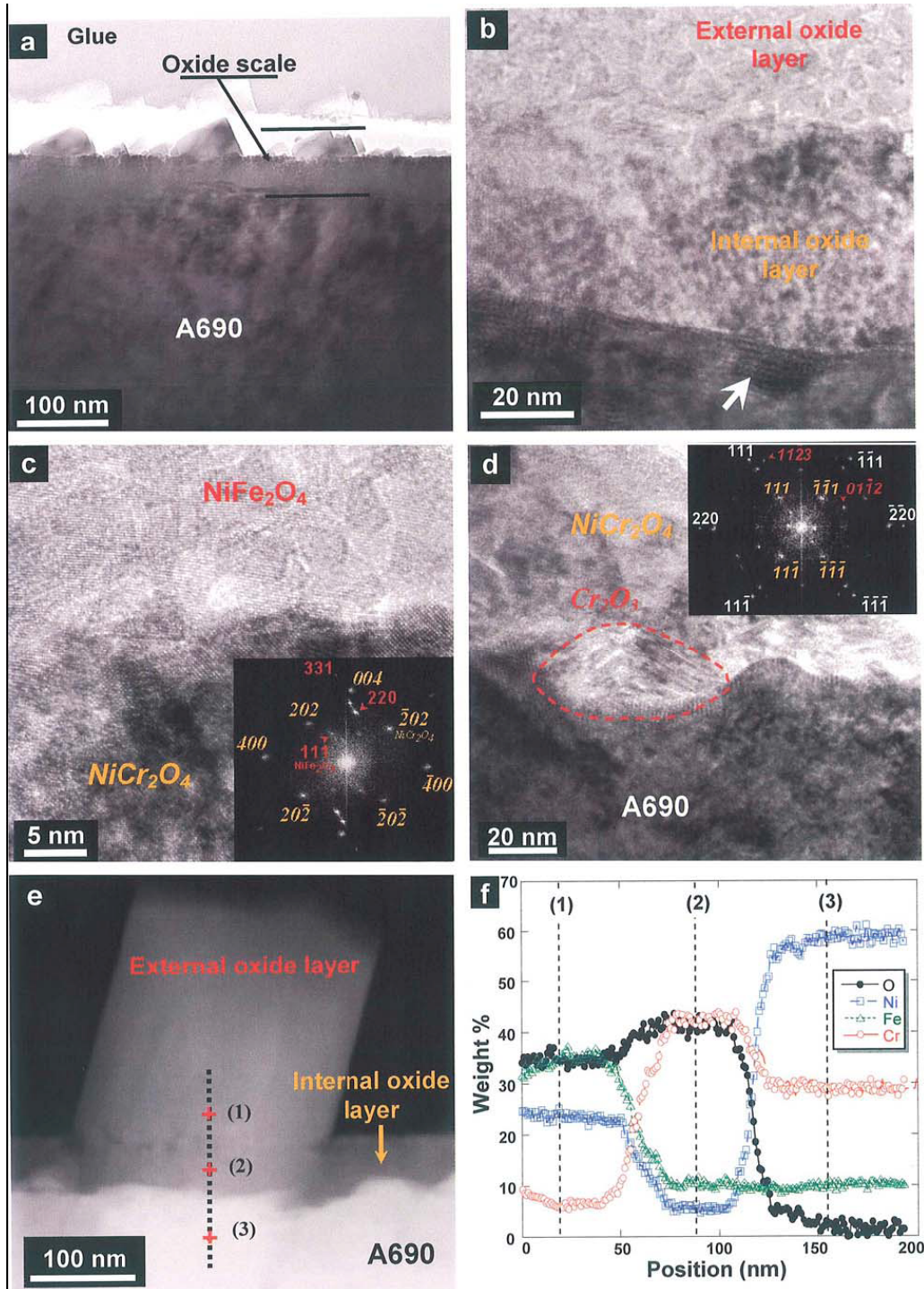
for Alloy 690 in PWR PW **saturated with Ni^{+2} and/or Fe^{+2}** the passive film consists of an inner layer of Cr_2O_3 /chromite, an intermediate layer of mixed-cation spinel, and an outer layer of nickel-ferrite. *(see next four slides)*

Alloy 690 in PWR PW sat'd with $\text{Ni}^{+2}_{\text{aq}}$ and $\text{Fe}^{+2}_{\text{aq}}$
i.e., lab tests conducted in stainless steel water loop and autoclave



**OXIDATION OF NI BASE ALLOYS IN PWR WATER:
OXIDE LAYERS AND ASSOCIATED DAMAGE TO THE BASE METAL**
P. Combrade¹, P.M. Scott², M. Foucault¹, E. Andrieu³, P. Marcus⁴

Proceedings of the 12th International Conference on
Environmental Degradation of Materials in Nuclear Power System – Water Reactors –
Edited by T.R. Allen, P.J. King, and L. Nelson TMS (The Minerals, Metals & Materials Society), 2005



Alloy 690 in PWR PW sat'd
with $\text{Ni}^{+2}_{\text{aq}}$ and $\text{Fe}^{+2}_{\text{aq}}$
i.e., lab tests conducted in stainless
steel water loop and autoclave

TEM (a) and HRTEM (b and c) images of the oxide layer developed on Alloy 690 exposed 858 h showing the large crystallites forming the external oxide layer and the continuous and compact internal layer. Analysis of image FFT diffractograms (inset in 6c) established the NiCr₂O₄-structure of the internal layer and the NiFe₂O₄-structure of the large crystallites

MOHAMED SENNOUR₍₁₎^{*}, LOÏC MARCHETTI₍₂₎, FRANTZ MARTIN₍₂₎,
STÉPHANE PERRIN₍₂₎, RÉGINE MOLINS₍₁₎, MICHÈLE PIJOLAT₍₃₎

Journal of Nuclear Materials, 2010, 402(2-3), 147-156,

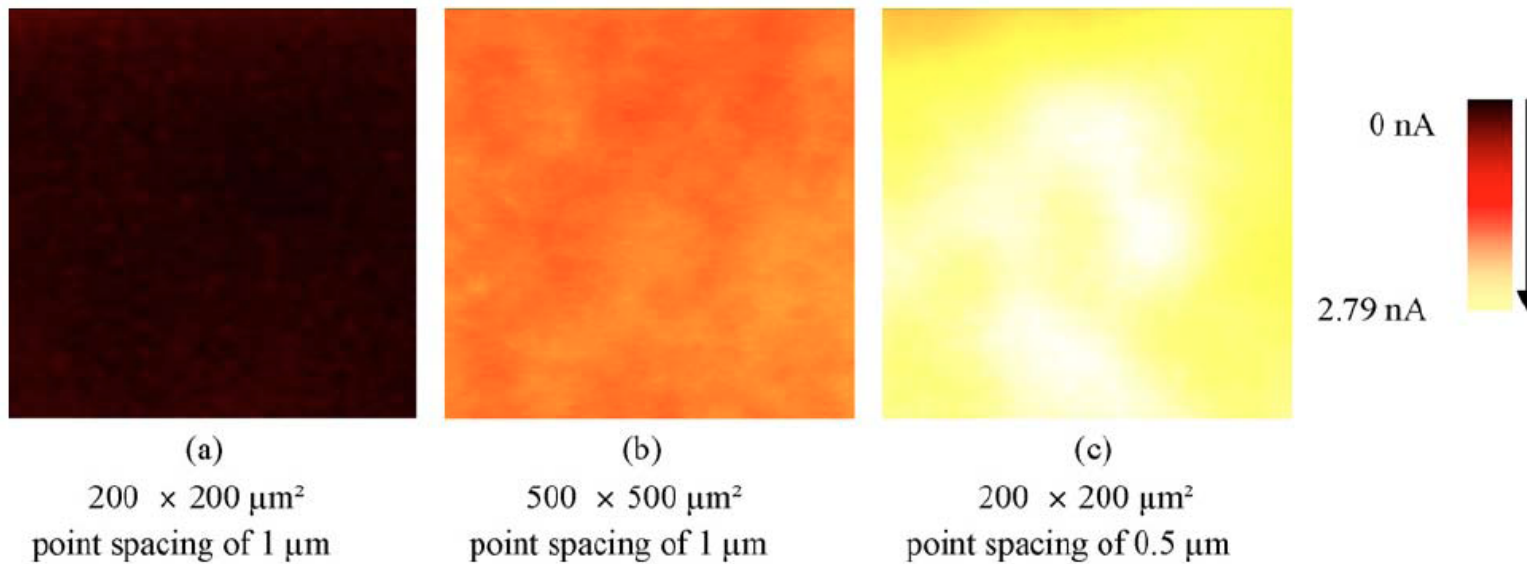


Figure 10: Photocurrent intensity mapping of alloy 690 samples corroded in PWR primary medium during (a) 48 h, (b) 406 h and (c) 858 h performed at a potential of 50 mV/MSE and a wavelength of 351 nm ($h\nu = 3.5 \text{ eV}$).

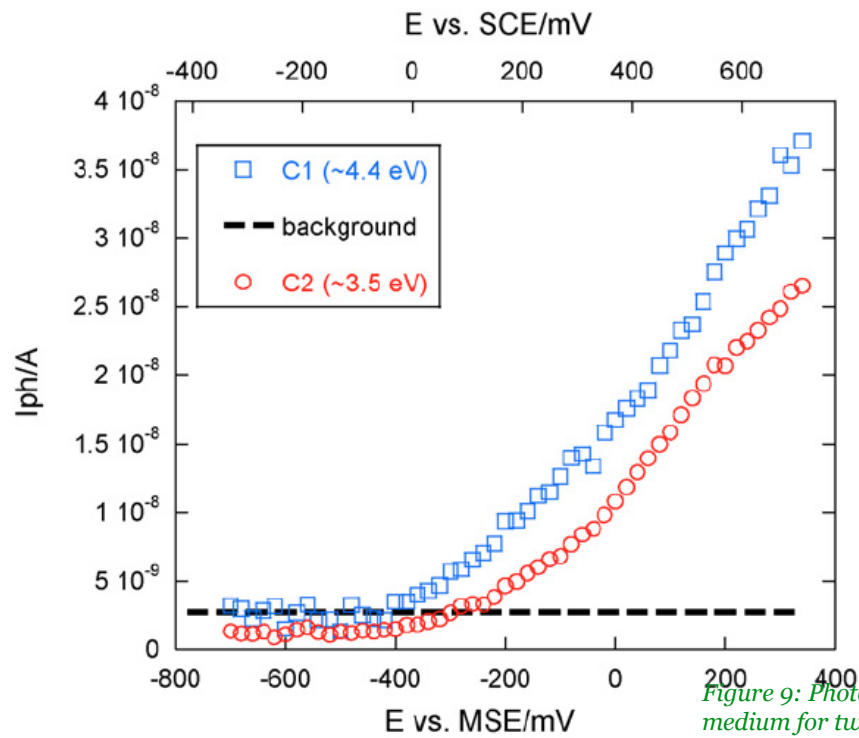


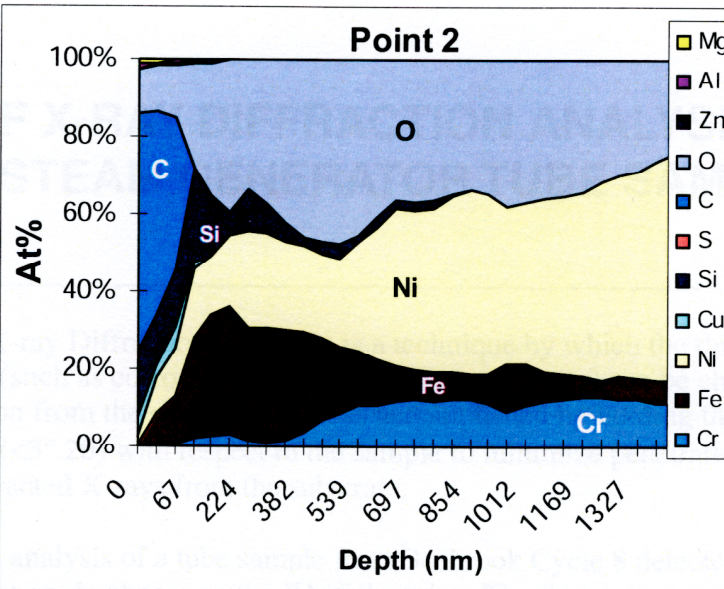
Figure 9: Photocurrent intensity in function of potential obtained for a sample corroded 858 h in PWR primary medium for two different light energies corresponding to C2 (~3.5 eV) and C1 (~4.4 eV).

Alloy 690 in PWR PW sat'd
with Ni^{+2}_{aq} and Fe^{+2}_{aq}
i.e., lab tests conducted in stainless
steel water loop and autoclave

LOÏC MARCHETTI⁽¹⁾, STÉPHANE PERRIN^{(1)*}, YVES WOUTERS⁽²⁾, MICHÈLE PIJOLAT⁽³⁾

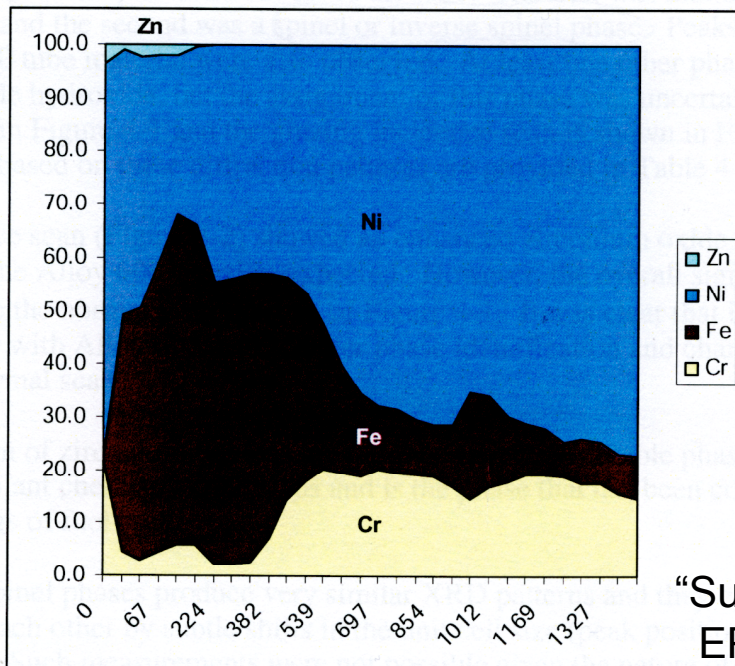
Electrochimica Acta, 2010, 55(19), 5384-5392,

A



Alloy 690 in PWR PW sat'd
with Ni^{+2} _{aq} and Fe^{+2} _{aq}
i.e., steam generator tubes

B



Cr-rich inner layer,
Low Cr in outer layer

Film on average =
 NiCrFeO_4

“Surface Analysis of PWR SG Tubing Specimens
EPRI 1018720, A. Parsi, A. Beyers, R.L. DeVito
J. Deshon Proj. Mngr. April 2009

Figure 3-26

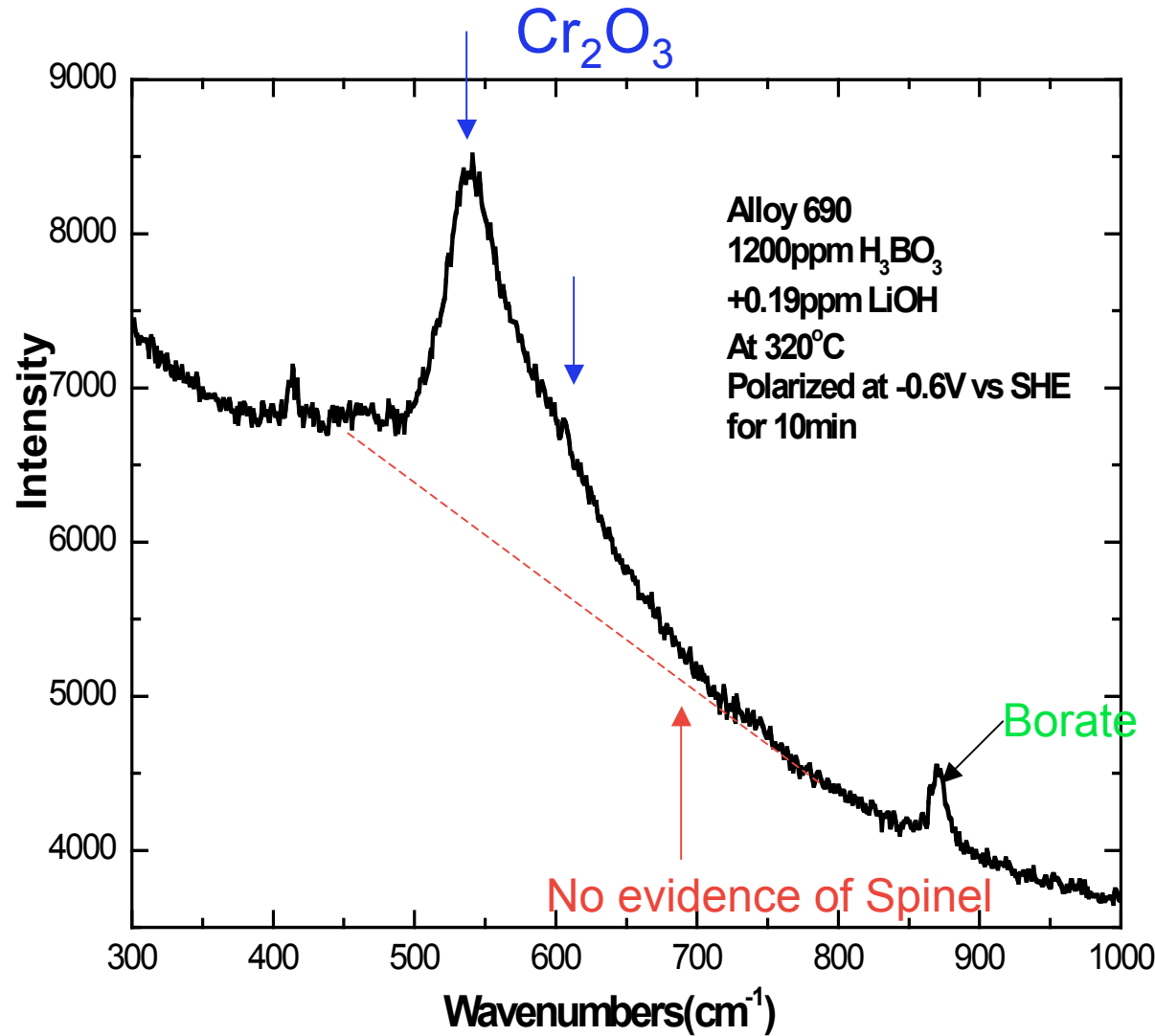
Farley 2 EOC 11 HL (R18-C42) Spot 2 AES Elemental Profile (A) Complete Element Atomic %, (B) Atomic % Normalized to Ni, Fe, Cr and Zn

Our analysis points out the critical role of aqueous metal cations on the structure and composition of Inner Layer of passive film

For Alloy 690 in PWR PW saturated with Ni^{+2} and/or Fe^{+2} the passive film consists of an inner layer of chromite, an intermediate layer of mixed-cation spinel, and an outer layer of nickel-ferrite.

**For Alloy 690 in PWR PW with $[\text{Ni}^{+2}]_{\text{aq}} \approx [\text{Fe}^{+2}]_{\text{aq}} \approx 0$, the passive film consists of a single layer of Cr_2O_3 .
(see *next slide*)**

Alloy 690 in PWR PW with $[Ni^{+2}_{aq}] = [Fe^{+2}_{aq}] = 0$
i.e., lab tests conducted in titanium autoclave with Ti water loop



Our analysis points out the critical role of aqueous metal cations on the structure and composition of Inner Layer of passive film.

Specifically,

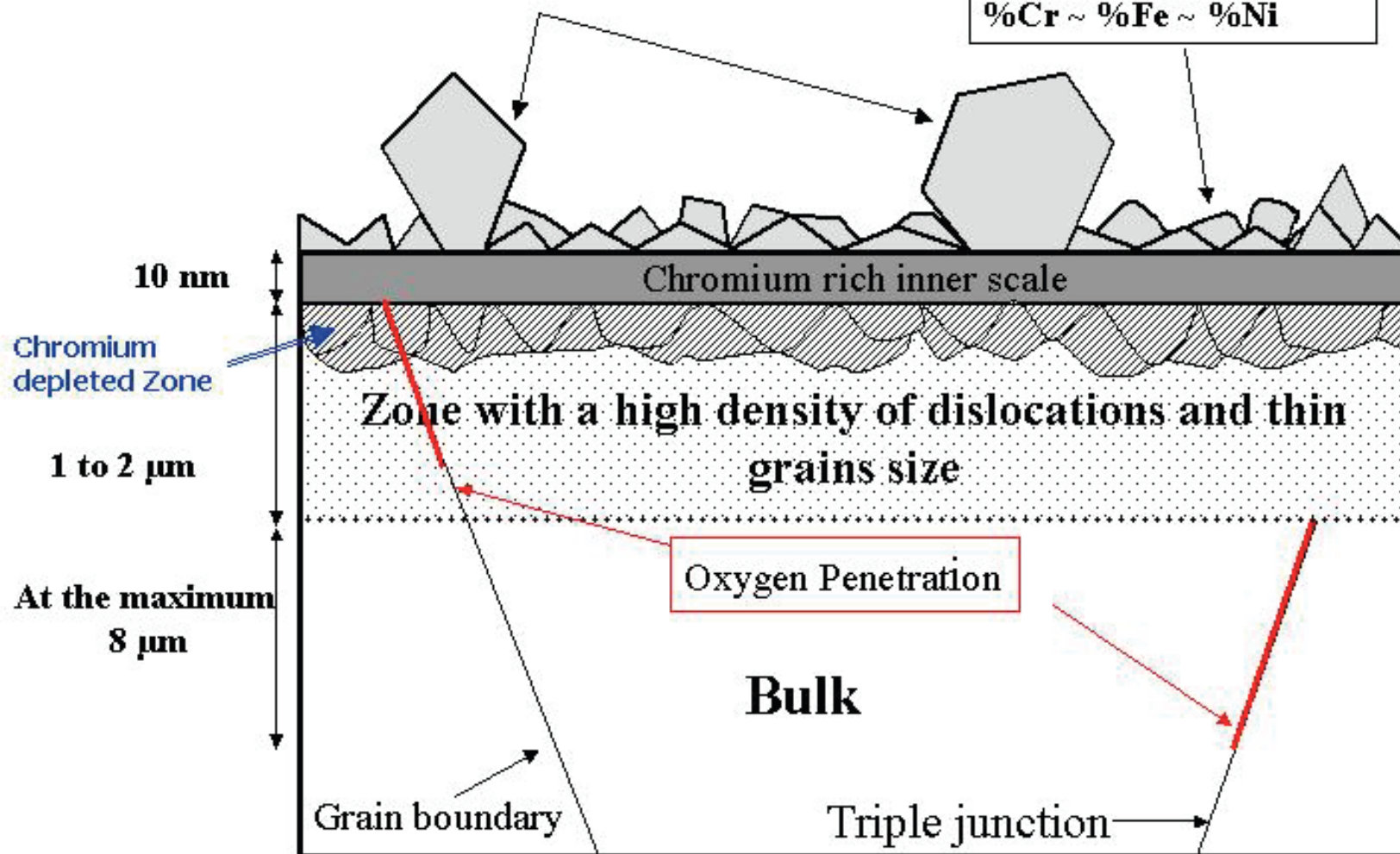
for Alloy 600 in PWR PW saturated with Ni^{+2} and/or Fe^{+2} the passive film consists of an inner layer of chromite, an intermediate layer of mixed-cation spinel, and an outer layer of nickel-ferrite. (*see next slide*)

Spinel oxides crystallites

$$\% \text{Cr} / \% \text{Ni} = f(\% \text{ Cr of alloy})$$

Oxyde ou hydroxyde ?

$$\% \text{Cr} \sim \% \text{Fe} \sim \% \text{Ni}$$



EFFECT OF THE CHROMIUM CONTENT AND STRAIN ON THE CORROSION OF NICKEL BASED ALLOYS IN PRIMARY WATER OF PRESSURIZED WATER REACTORS

F. Delabrouille^{1,3}, L. Legras¹, F. Vaillant¹, P. Scott², B. Viguier³, E. Andrieu³

Proceedings of the 12th International Conference on Environmental Degradation of Materials in Nuclear Power System – Water Reactors – Edited by T.R. Allen, P.J. King, and L. Nelson TMS (The Minerals, Metals & Materials Society), 2005

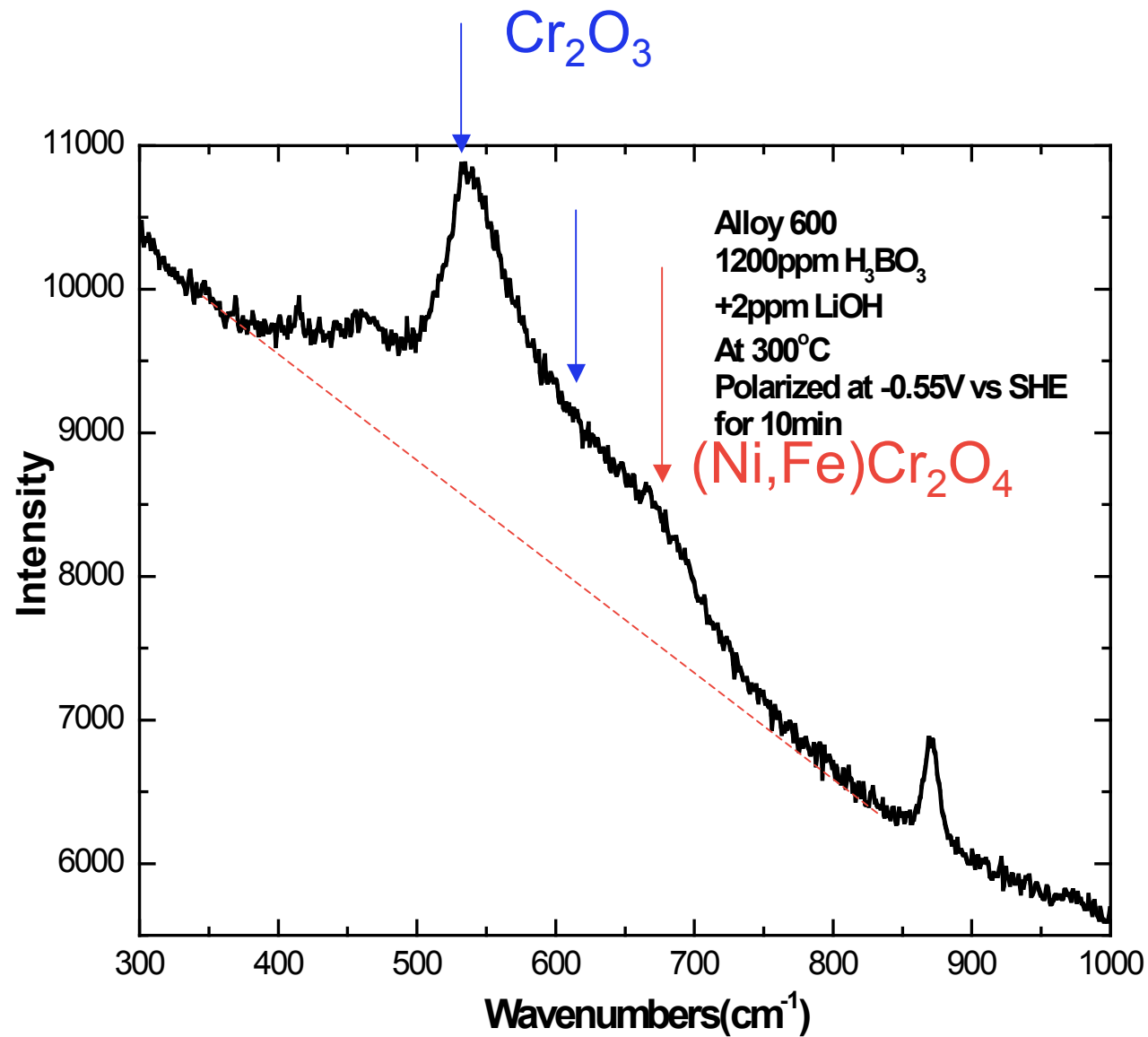
Our analysis points out the critical role of aqueous metal cations on the structure and composition of Inner Layer of passive film.

Specifically,

for Alloy 600 in PWR PW saturated with Ni^{+2} and/or Fe^{+2} the passive film consists of an inner layer of chromite, an intermediate layer of mixed-cation spinel, and an outer layer of nickel-ferrite.

For Alloy 600 in PWR PW with $[\text{Ni}^{+2}]_{\text{aq}} \approx [\text{Fe}^{+2}]_{\text{aq}} \approx 0$, the passive film consists of an inner layer of Cr_2O_3 and an outer layer of mixed cation spinel (no layer of nickel-ferrite)
(see next slide)

Duplex film forms on Alloy 600 in PWR PW w/o aqueous cations
i.e., lab tests conducted in titanium autoclave and water loop



F. Wang and T.M. Devine (2010)

Note that the distribution of photocurrent indicates that Cr₂O₃ is everywhere except at the few black dots. This indicates that the Cr₂O₃ film is continuous, at least on the scale of 1 μm .

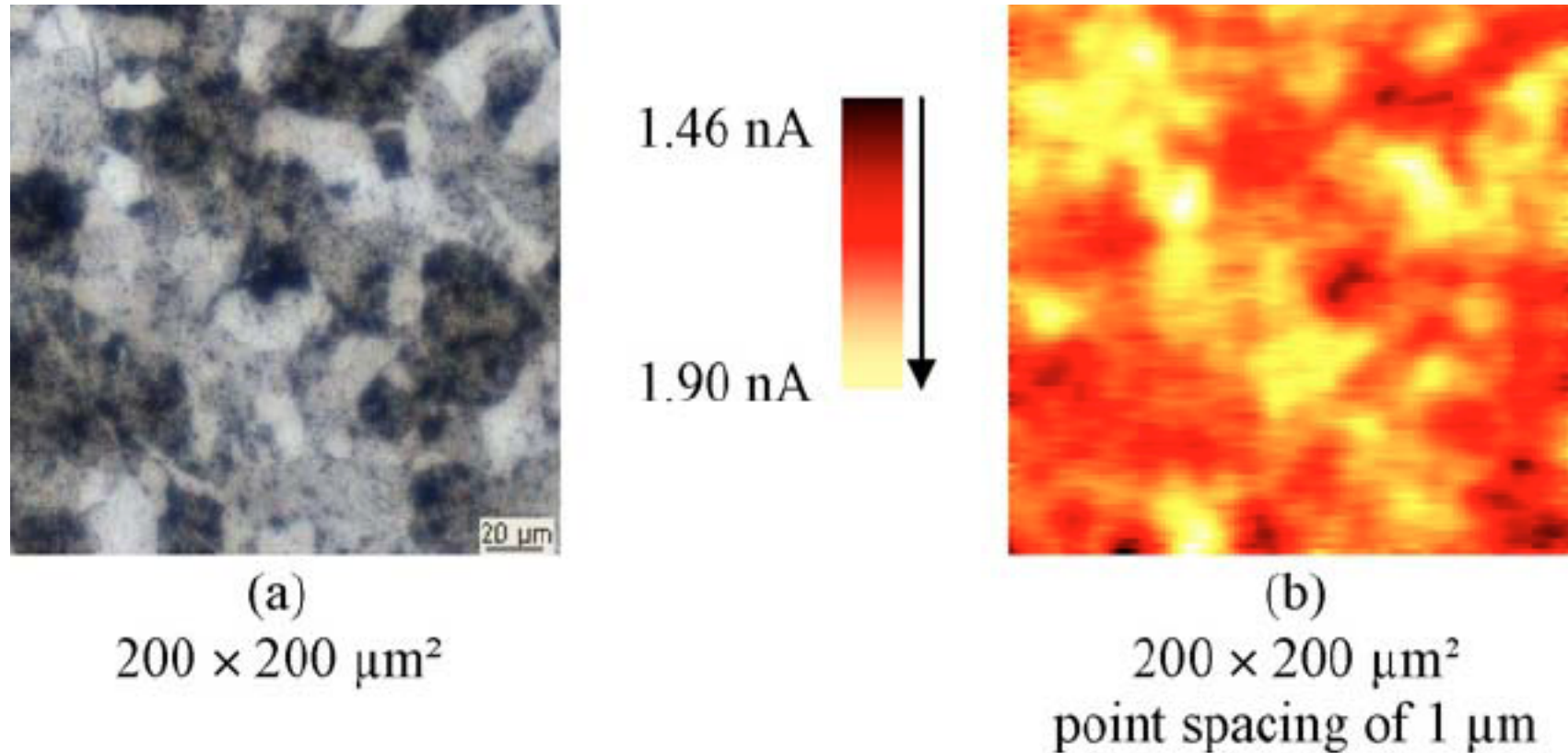


Figure 11: Optical image (a) and associated photocurrent intensity mapping (b) of alloy 600 sample corroded in PWR primary medium during 858 h performed with a potential of 50 mV/MSE and a wavelength of 351 nm ($h\nu = 3.5 \text{ eV}$).